The Cost of Irreversible and Uncertain Climate Tipping Points[*]

Andrea Titton[†]

November 1, 2024

Find latest version here.

Abstract

Climate tipping points are abrupt, irreversible shifts in the climate system potentially locking the world into a high-temperature regime that is difficult or not possible to reverse. This paper examines the economic consequences of such tipping points, focusing on the costs associated with their unpredictability. Using an integrated assessment model with a climate system exhibiting a tipping point, I compute optimal abatement policies under the assumptions that the tipping point is either imminent or remote. To bound the economic cost of the uncertainty in the tipping point, I compare two scenarios: one where a *wishful thinker* planner erroneously assumes the tipping point is remote and delays abatement, and another where a *prudent* planner assumes incorrectly that the tipping point is imminent. I show that the cost of uncertainty in tipping points can reach up to 32% of current global output. Moreover, I find that in the face of uncertainty, prudence, while costly, is more cost effective than delaying abatement. Abatement policies should hence err on the side of caution.

As the global average temperature rises due to greenhouse gas emissions from human activities, temperature feedback mechanisms in the climate system can drive the world past critical thresholds, known as tipping points, into a regime of high temperatures. These tipping points pose two challenges to determining optimal abatement strategies that try to balance current benefits of emissions and resulting future climate damages. First, tipping points cannot be predicted by just observing historical data (Ben-Yami et al., 2024), giving policymakers little time to react once they are detected. Second, as crossing a tipping point triggers a new, possibly irreversible, climate regime, climate damages suddenly increase. This discontinuity implies that evaluating optimal abatement policies using marginalist analysis, such as the social cost of carbon, can lead policy makers astray.

In this paper, I study the economic costs of unpredictable and irreversible climate tipping points. Using an integrated assessment model that incorporates temperature feedback effects, I compute optimal abatement strategies under two different scenarios: one where a tipping point is imminent and one where it is remote. These scenarios are calibrated to reflect extreme cases from the climate literature (Armstrong McKay et al., 2022; Seaver Wang et al., 2023). I then compute an upper bound on the economic costs of tipping points through two experiments. The first measures the cost incurred by a *wishful thinker* social planner who mistakenly assumes the tipping point is remote, delaying optimal abatement until after it is crossed. This serves as an upper bound on the cost of under-abating. The second considers a *prudent* planner who incorrectly assumes the tipping point is imminent, leading to more aggressive abatement. This serves as an upper bound on the cost of over-abating. Together, these scenarios provide an upper bound on the economic costs of tipping, without requiring prior assumptions about the tipping point's exact location and avoiding marginalist calculations, which are ill-defined in the presence of tipping points. Furthermore, the excess cost incurred in the two scenarios, compared to the optimal policies, is an estimate of the cost of uncertainty. This can be seen

2

as the price society would be willing to pay to discover the tipping point and switch to an optimal abatement strategy.

I show that the cost of uncertainty in tipping points can be as large 26.25 trillions US $ per year or approximately 32 % of current world output. Reacting to this uncertainty by prudence and minimising the risk of tipping requires quick abatement efforts, which incur large adjustment costs. Reacting to this uncertainty by wishful thinking and delaying abatement, locks the world with high chance into a hot regime characterised by large climate damages. Both are very costly approaches, yet wishful thinking can cost up to 3.22 trillions of US $ per year more than prudence. Hence, when faced with uncertainty, it is cheaper for policymakers to tread with caution.

The rest of the paper is structured as follows. Section 1 puts the current paper in the context of the climate and environmental economic literature and highlights its contributions. Section 2 presents a stylised version of the model with a temperature feedback that generates an irreversible tipping point. This simplified model serves as illustration of the major challenges faced in computing optimal abatement when faced with a tipping point, which carry over in the extended model used for calibration. The components of the extended model are then introduced in Section 3: the climate, the economy, and the social planner problem. Section 4 computes optimal abatement policies when tipping points are known. Section 5 introduces the *wishful thinker* and *prudent* social planner problem and computes the economic damages from tipping points and the cost of uncertainty. Finally, Section 6 draws policy implications and concludes.

1   Related Literature

A large recent literature in economics has highlighted the importance of correctly incorporating climate dynamics when analysing the economic trade-off between current emissions and the reduction of future temperature induced climate damages. The key challenge is to develop integrated assessment models

that, on the one hand, are sufficiently simple to be integrated into a dynamic optimisation problem, necessary to compute the economic costs of climate change and optimal abatement policies, and, on the other hand, are able to reproduce the key dynamics of larger, more accurate climate models (Dietz et al., 2020). One feature of the climate that has drawn a lot of attention in economics are climate tipping points (Li, Crépin and Lindahl, 2024).

Early work dealing with uncertain tipping points in environmental economics (Kamien and Schwartz, 1971; Nævdal and Oppenheimer, 2007; Tsur and Zemel, 1996, among others) has modelled tipping points via stochastic jump processes. Henceforth, I refer to this approach as *Barro style disasters* as it builds on work on economic catastrophes by Barro (2009). At each moment in time, either temperature or atmospheric carbon concentration experiences a discontinuous jump with some probability known to the planner. This approach was introduced to climate economics by Pindyck and Wang (2013). It has been used in modelling climate tipping points by, for example, Lontzek et al. (2015), Cai, Lenton and Lontzek (2016), and Van Der Ploeg and De Zeeuw (2018). Its wide adoption is due to its flexibility, as it allows one to readily incorporate ambiguity concerns (Lemoine and Traeger, 2016), learning (Lemoine and Traeger, 2014), and self exciting processes (Hambel, Kraft and Schwartz, 2021). Furthermore, it is analytically tractable and can be used to derive closed form approximations for the contribution of tipping points to the social cost of carbon (Li, Crépin and Lindahl, 2024; Lin and van Wijnbergen, 2023; Van den Bremer and Van der Ploeg, 2021). Nevertheless, this modelling choice lacks two crucial features that are the focus of this paper. First, climate tipping points can introduce different temperature regimes. Barro style disasters are not suited to model these different regimes as they simply model single transient catastrophic events. Second, it requires defining a probability distribution on the tipping event, be that real or the belief of the social planner.

Another approach is to model feedback in the climate dynamics explicitly. Henceforth, I refer to this as the *feedback approach*. This is closer to the real

behaviour of the climate system (McGuffie and Henderson-Sellers, 2014), as it introduces multiple climate regimes, and is the standard one adopted in more complex climate modelling (e.g. Smith et al. 2017). Furthermore, optimisation over such systems has a long history in economics (Skiba, 1978) and has been developed extensively in environmental economics (Mäler, Xepapadeas and de Zeeuw, 2003; Wagener, 2013) and, specifically, in climate economics (Greiner and Semmler, 2005; Nordhaus, 2019; Wagener, 2015). Modelling the feedback explicitly has one drawback: it requires assuming the size of the feedback and when it kicks in. These two facts are objects of contention (Armstrong McKay et al., 2022; Seaver Wang et al., 2023). Because of this, the feedback approach has not been widely employed in the climate economic literature, especially when trying to give quantitative estimates of costs via calibration.

In this paper, I bridge these two approaches. By embedding and calibrating a temperature feedback in a state of the art dynamic stochastic general equilibrium model with a climate component, I obtain empirical estimates of the costs of uncertainty of tipping points. The focus of the two extreme scenarios, a *wishful thinker* and a *prudent* planner, allows me to obtain an upper bound on the cost of under-abating and suffering climate damages and over-abating and paying large adjustment costs. These serve then as an upper bound for the overall cost of tipping points. Despite being only upper bounds, these estimates do not require an arbitrary prior on the tipping point and can be computed in a scenario of multiple climate regimes.

Finally, the numerical solver developed in the paper contributes to the literature on controlled stochastic processes by developing a parallelisation algorithm, based on Bierkens, Fearnhead and Roberts (2019), for the class of solver introduced in Kushner and Dupuis (2001), and extending their results to recursive utilities.

2 Stylised Example

Before turning to the extended model in the next section (3), in what follows I discuss a stylised integrated assessment model with an irreversible tipping point. The climate has a more stylised temperature feedback compared to the extended model. In addition, the planner objective is reduced to a simple optimal stopping problem. Despite its simplicity, this stylised model illustrates the two main challenges tipping points pose to the computation of optimal abatement. First, their unpredictability hinders evaluation of future damages. Second, their irreversibility makes analyses based on marginal emission benefits and marginal temperature damages misleading.

Emissions of CO_2 from human economic activity E_t $[Gt\,CO_2]$ raise CO_2 atmospheric concentration M_t [p.p.m.],

$$\frac{dM_t}{dt} = \xi_m E_t \tag{1}$$

where ξ_m converts $Gt\,CO_2$ to p.p.m.. As CO_2 is a greenhouse gas, an increase in its concentration M_t compared to the pre-industrial levels M^p, in turn, increases average temperature in deviation from the pre-industrial level T_t [°]. The change in temperature is given by

$$\frac{dT_t}{dt} = G_1 \log\left(\frac{M_t}{M^p}\right) - \lambda T_t, \tag{2}$$

where G_1 is the size of the greenhouse gas effect and λ is a stabilisation rate of temperature[1]. In this model, temperature tends towards the equilibrium

$$T_t \to \frac{G_1}{\lambda} \log\left(\frac{M_t}{M^p}\right) \text{ as } t \to \infty, \tag{3}$$

that is, the equilibrium temperature grows as the logarithm of atmospheric carbon concentration.

Consider a social planner who derives utility $u(E_t)$ from CO_2 emissions E_t

---

[1]Throughout this section, I assume for illustration purposes $G_1 = 1$, $\xi_m = 1$, and $\lambda = 1$.

and disutility $d(T_t)$ from temperature T_t, and discounts both at a rate ρ. For simplicity assume the emissions are constant at a level $\bar{E}$, such that CO_2 concentration grows linearly $M_t = M^p + (\xi_m \bar{E}) t$, and the social planner needs to decide at what time τ society ought to stop emitting. At that point society loses the benefits of emissions $u(\bar{E})$ and pays the damages of the resulting temperature $d(T_\tau)$. To summarise, the planner is trying to maximise

$$J(\tau) := (1 - e^{-\rho\tau})\, u(\bar{E}) - e^{-\rho\tau}\, d(T_\tau) \tag{4}$$

by choosing an emission stopping time $\tau \geq 0$. This problem is readily solved by a marginalist planner: the time τ to stop emissions is when the marginal utility of an additional instant of emissions does not justify the marginal increase in temperature damages, or $\partial J/\partial \tau = 0$.

Unfortunately, unlike the stylised model in equation (2), the climate system is more complex: there are many temperature feedbacks that can generate tipping points (Seaver Wang et al., 2023). Consider, for example, the the ice-albedo feedback (Riihelä, Bright and Anttila, 2021). As carbon concentration warms the planet, large bodies of ice melt, such as the west Antarctic or Greenland ice sheets. This reduces the surface albedo, that is, the fraction of solar radiation reflected by the earth surfaces, which further contributes to warming. This feedback can generate a low temperature regime, in which the ice has not melted and the albedo is high, and a high temperature regime, in which the low albedo prevents ice from reforming. If a tipping point is crossed, all ice melts and the earth is a trapped in a warmer regime. The amount of cooling needed for the ice to reform and hence restore the pre-tipping albedo is larger than the warming that melted the ice in the first place. Another possible feedback is that of the carbon release from thawing permafrost (Turetsky et al., 2019). Warming is causing frozen soils to thaw and microorganisms start breaking down matter in the soil, which in turn releases greenhouse gasses into the atmosphere. Importantly, both of these examples have two features which are not captured in the economic literature: they are hard to predict and are de facto irreversible.

One way to introduce these into the toy model is to assume the stabilisation rate λ is a function of average temperature T_t. In this case, the change in temperature (2) is given by[2]

$$\frac{\mathrm{d}T_t}{\mathrm{d}t} = G_1 \log\left(\frac{M_t}{M^p}\right) - \overbrace{\lambda(T_t)}^{\text{Feedback}} T_t. \tag{6}$$

Figure 1 shows the change in temperature $\mathrm{d}T_t / \mathrm{d}t$ as a function of temperature T_t when carbon concentration is at its pre-industrial level (left panel), 50% larger (middle panel) and twice as large (right panel). As in the model with-
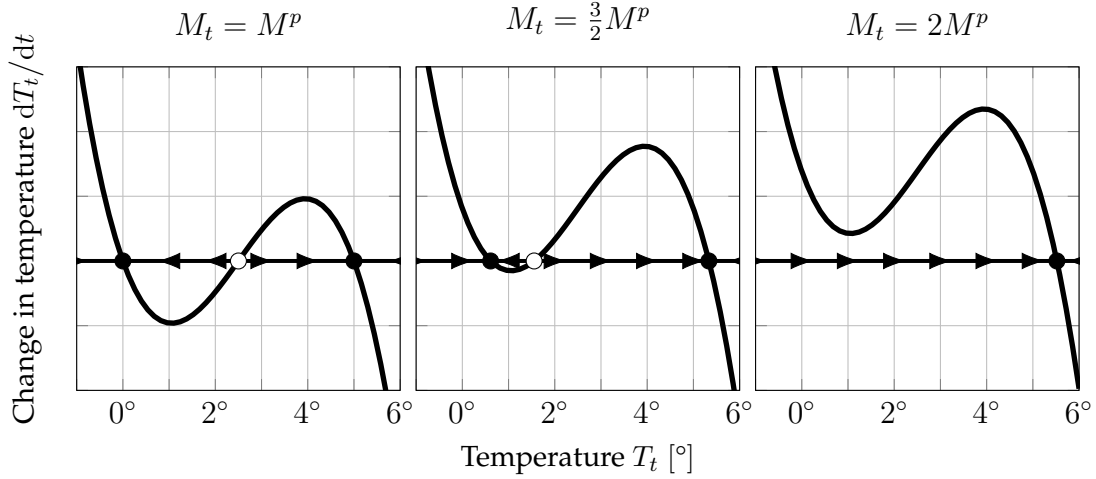

Figure 1: Change in temperature over time $\frac{\mathrm{d}T_t}{\mathrm{d}t}$ as a function of temperature T_t for three levels of atmospheric carbon concentration. The marker represents the equilibrium and the arrows indicate whether temperature is increasing (right) or decreasing (left).

out feedback (2), if carbon concentration is at its pre-industrial level (left panel) there is low temperature equilibrium $T_t \to 0°$ (low temperature black marker). In addition to this, a new high temperature equilibrium is formed $T_t \to 5°$ (high temperature black marker). In this high temperature equilibrium, the feedback has trapped temperature into a high regime, for example, an ice free world with

---

[2]For illustration purposes, in this section I assume

$$\lambda(T_t) = aT_t^2 - 3\sqrt{\frac{c}{a}}T + 2c \tag{5}$$

where $c = 1/2$ is a scale parameter and $a = 0.08$ is the intensity of the feedback. Any $\lambda(T_t)$ increasing in T_t would display the same multiplicity of equilibria (Murdock, 2003).

low albedo. As carbon concentration increases (from left to right panel), the average temperature raises. Yet, unlike in the case without feedback, the system goes through a tipping point[3]: the low temperature equilibrium becoming unfeasible triggers a sudden rise in temperature as it converges to the higher equilibrium. This phenomenon poses two problems from the point of view of the social planner trying to evaluate the trade-off between current emissions and future climate damages. First, if the temperature dynamics (6) are uncertain, one cannot hope to learn them from simply observing the path of temperature (Ben-Yami et al., 2024). To illustrate this, Figure 1 shows the path of temperature over time under constant emissions with (dark) and without (light) temperature feedback. The two trajectories are in contact, until the tipping point
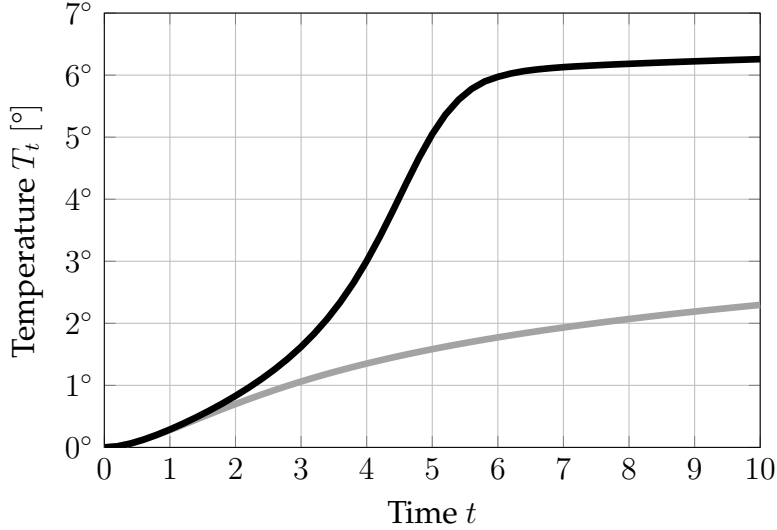

Figure 2: Path of temperatures given by (6), assuming constant emissions $E_t = \bar{E}$ with (dark) and without (light) temperature feedback.

is reached. After crossing it, they rapidly diverge. A planner attempting to determine whether the system has a tipping point by simply observing the temperature trajectory, would be unable to do so until the tipping point is reached. Second, marginalist calculations are not sufficient to solve the emission stopping problem given in equation (4). As mentioned above (Figure 1), the equilibrium temperature T_τ reached after τ time emitting can take on two possible value: a high or a low one. As a consequence, the social utility $J(\tau)$ of emitting

---

[3]This is a saddle-node bifurcation.

for τ time can also take two values depending in which temperature regimes the planner is. The objective J for different stopping times τ in the low and high temperature regimes is shown in grey and black, respectively, in Figure 3. In the low temperature regime, delaying abating emissions is optimal, as the
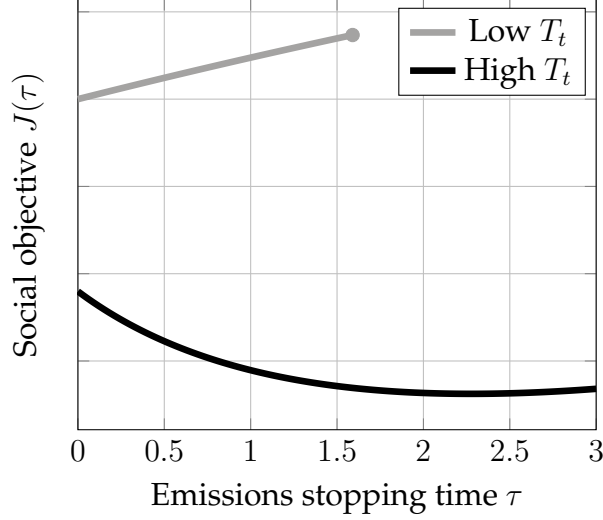

Figure 3: Social objective J (4) as a function of the emission stopping time τ, under a climate with temperature feedback (6).

marginal benefits of emissions are greater than the marginal climate damages (the lighter branch of J is always increasing). Yet by delaying abatement, the climate is brought closer to a tipping point (marker). At that point, marginal damages are not defined as any further delay to stopping emissions pushes the climate into the high temperature regime. The costs of tipping are hence not internalised in the marginal $\partial J / \partial \tau$. Once the system has tipped, the objective is given by the lower, darker line. After tipping, it is not possible to system cannot be reverted back to the low temperature equilibrium. In this new regime (black line) the planner wish he had stopped as early as possible, as J is maximised for $\tau = 0$.

This simple example illustrates how tipping points hinder the computation of optimal emissions by their marginal benefits and marginal damages. When the tipping point is hard to predict the path of marginal damages is uncertain. When the tipping point is irreversible the marginal damages are ill-defined along some of these paths.

3 Model

The following extends the stylised model from Section 2. First, Section 3.1.1 introduces carbon sinks and their interaction with atmospheric carbon concentration. Then, Section 3.1.2 presents the temperature dynamics and the feedback. Section 3.1.3 discusses the resulting tipping point in the climate system. Finally, Section 3.2 presents the Harrod–Domar economy.

3.1 Climate Model

3.1.1 CO_2 concentration and carbon sinks

Emissions from human economic activity E_t increase the atmospheric concentration of CO_2 M_t. Part of this, in turn, decays into natural sinks N_t. The rate of decay $\delta_m(N_t)$ falls in the quantity of carbon dioxide already stored in the natural sinks N_t, as the sinks saturate (Le Quéré et al., 2007; Shi et al., 2021). Hence, the stored carbon evolves as

$$\xi_m \, dN_t = \delta_m(N_t)M_t \, dt \tag{7}$$

where ξ_m converts $\mathrm{Gt}\, CO_2$ to p.p.m..

In absence of abatement efforts, the atmospheric concentration of CO_2 M_t evolves according to the *business-as-usual* SPSS5 scenario (Kriegler et al., 2017). Variables under this scenario are indexed by b: let E_t^b be the business-as-usual emissions, and M_t^b and N_t^b the resulting atmospheric carbon concentration and carbon stored in natural sinks, respectively. The business-as-usual atmospheric carbon concentration M_t^b evolves as

$$\frac{dM_t^b}{M_t^b} = \gamma_t^b \, dt + \sigma_m \, dW_{m,t} \tag{8}$$

where the business-as-usual growth rate of atmospheric carbon concentration is given by

$$\gamma_t^b := \xi_m \frac{E_t^b}{M_t^b} - \delta_m(N_t^b) \tag{9}$$

11

and $W_{m,t}$ is a Wiener process. This scenario describes an energy intensive future, in which fossil fuel usage develops rapidly and little to no abatement takes place. Using the projected carbon concentration path M_t^b from Kriegler et al. (2017), I calibrate the implied growth rate of carbon concentration γ_t^b. The calibration is described in Appendix C and its results are shown in Figure 4. The
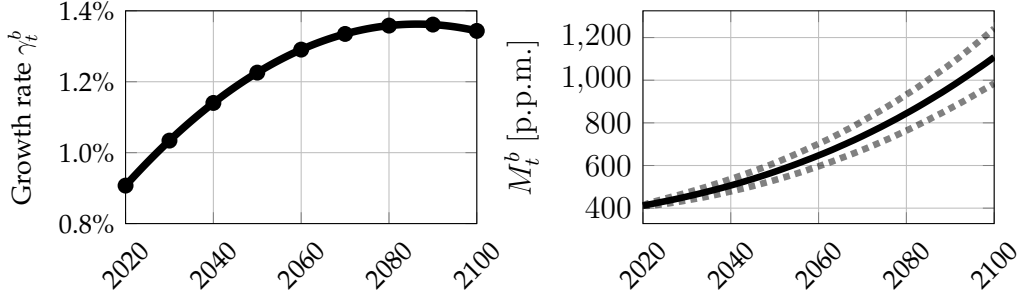

Figure 4: Growth rate of carbon concentration in the business-as-usual scenario γ_t^b and median path (solid) of business-as-usual carbon concentration M_t^b (8) with 95% simulation interval (dashed).

left figure shows the path of the business-as-usual growth rate γ_t^b and the right figure shows the resulting growth of carbon concentration M_t^b. The carbon concentration in this scenario grows at an increasingly fast rate until 2080, when the growth rate peaks just below 1.4%. Thereafter, the growth rate starts declining.

Abatement efforts α_t lower the growth rate of carbon concentration M_t vis-à-vis the business-as-usual scenario M_t^b. That is, the growth rate of carbon concentration M_t satisfies

$$\frac{\mathrm{d}M_t}{M_t} = \left(\gamma_t^b - \alpha_t\right)\mathrm{d}t + \sigma_m\,\mathrm{d}W_{m,t} \tag{10}$$

where $\mathrm{d}W_{m,t}$ is a Wiener process. Not implementing any abatement policy $\alpha_t = 0$ corresponds to a business-as-usual scenario $M_t = M_t^b$, while implementing a full abatement policy $\alpha_t = \gamma_t^b$ stabilises carbon concentration. Any abatement policy α_t can be implicitly linked back to the corresponding level of emissions by introducing the emission reduction rate $\varepsilon(\alpha_t)$, which keeps tracks of what fraction of emission has been abated

$$E_t = \left(1 - \varepsilon(\alpha_t)\right)E_t^b. \tag{11}$$

In this paper I assume that the planner does not have access to carbon capture technology. This is implemented by imposing that abatement cannot exceed the growth rate of carbon concentration and the carbon decay into natural sinks, namely

$$\alpha_t \leq \gamma_t^b + \delta_m(N_t). \tag{12}$$

Hence, if no abatement efforts are undertook $\alpha_t = 0$, no emissions are abated $\varepsilon(0) = 0$ and $E_t = E_t^b$. If abatement efforts are maximal $\alpha_t = \gamma_t^b + \delta_m(N_t)$, net zero emissions are reached $\varepsilon(\gamma_t^b + \delta_m(N_t)) = 1$ and $E_t = 0$.

3.1.2 Temperature

Average world temperature is determined by a zero dimensional energy balance model (McGuffie and Henderson-Sellers, 2014, p.85). Earth's radiating balance, in its simplest form, prescribes that temperature tends towards balancing incoming solar radiation S and outgoing long-wave radiations $\eta\sigma T^4$, where σ is the Stefan-Boltzmann constant and η is an emissivity rate. Due to the presence of greenhouse gasses, certain wavelengths are scattered and, hence, not emitted (Ghil and Childress, 2012). This introduces an additional radiative forcing G which yields the balance equation $S = \eta\sigma T^4 - G$. Focusing on the role of increased CO_2, as opposed to other greenhouse gases, we can decompose the greenhouse radiative forcing term G into a constant component G_0 and a component which depends on the equilibrium level of CO_2 concentration in the atmosphere M_t with respect to the pre-industrial level M^p, such that

$$G = G_0 + G_1 \log(M_t/M^p). \tag{13}$$

I introduce a feedback in the temperature by assuming that the absorbed incoming solar radiation is increasing in temperature. This choice can be seen as a stylised model of the ice-albedo feedback (Ashwin et al., 2012; McGuffie and Henderson-Sellers, 2014), yet, any temperature feedback in temperature dynamics yields a similar interpretation. Hence, incoming solar radiation S

can be decomposed as $S_0\left(1 - \lambda(T_t)\right)$ where the function $\lambda(T_t)$ transitions from a higher λ_1 to a lower level $\lambda_1 - \Delta\lambda$ via a smooth transition function $L(T_t)$. To control at which level of temperature the transition occurs the transition functions take the form

$$\lambda(T_t) := \lambda_1 - \Delta\lambda\big(1 - L(T_t)\big) \text{ where} \tag{14a}$$

$$L(T_t) := \frac{1}{1 + \exp\left(-L_1\left(T_t - T^c\right)\right)} \tag{14b}$$

where T^c [°] is the level of temperature at which the feedback kicks in and L_1 is a speed parameter.

The threshold temperature T^c determines the horizon at which the feedback effect kicks in. Best estimates from climate sciences are that many such transitions occur for temperatures T_t between $1.5°$ and $3°$ over pre-industrial levels (Armstrong McKay et al., 2022; Seaver Wang et al., 2023). A large body of literature has focused on estimating critical thresholds associated with climate tipping points (e.g. Boulton, Allison and Lenton 2014; Van Westen, Kliphuis and Dijkstra 2024). Yet, for many climate feedback mechanisms either the uncertainty is too large (Ben-Yami et al., 2024) or it is not theoretically possible to (Ditlevsen and Johnsen, 2010; Wagener, 2013) compute their tipping points. In line with this, to avoid attaching an arbitrary prior over a critical threshold T^c, in this paper I choose to focus on two extreme scenarios: one in which the tipping point is *imminent* $T^c = 1.5°$ and one in which it is *remote* $T^c = 2.5°$. The parameter $\Delta\lambda$ is calibrated by matching the equilibrium climate sensitivity, that is, the expected equilibrium temperature of doubling pre-industrial level CO_2 concentration, of $4.5°$, which is the upper end of the range deemed very likely in AR6 (IPCC, 2023). Figure 5 shows the transition function (14) under these two scenarios. Despite being a highly stylised and reduced form representation of a complex and spatially heterogeneous process, λ captures the core mechanism behind feedback processes in the temperature dynamics that can generate tipping points (McGuffie and Henderson-Sellers, 2014). This simple temperature feedback allow us to discuss and estimate the costs of ending in a new regime,
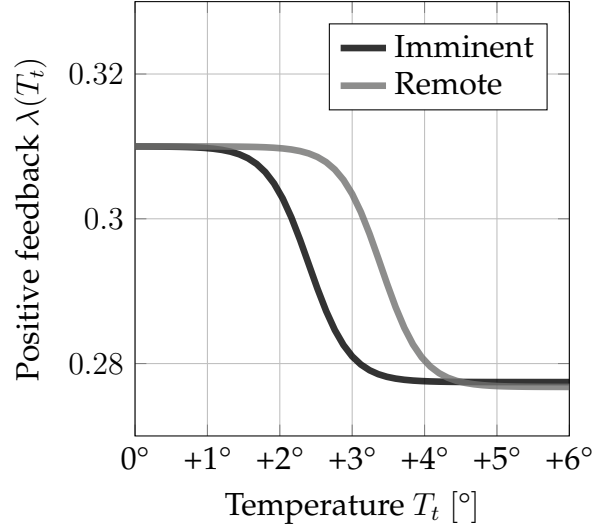
Figure 5: Temperature feedback $\lambda(T_t)$ in the *imminent* and the *remote* scenario.

what ought to be (or not be) done to prevent this from happening, and the cost associated with their uncertainty.

Putting these processes together we can write the two determinants of temperature dynamics: radiative forcing, which only depends on temperature,

$$r(T_t) \coloneqq S_0 \left(1 - \lambda(T_t)\right) - \eta \sigma T_t^4 \tag{15}$$

and the greenhouse gas effect, which only depends on atmospheric carbon concentration

$$g(M_t) \coloneqq G_0 + G_1 \log(M_t/M^p). \tag{16}$$

Under these two drivers, temperature changes are given by

$$\epsilon \, dT_t = r(T_t) \, dt + g(M_t) \, dt + \sigma_T \, dW_{T,t}, \tag{17}$$

where ϵ is the thermal inertia and $W_{T,t}$ is a Wiener process.

3.1.3 Tipping Points

The presence of the temperature feedback λ introduces a tipping point. In the following, I discuss the consequences of this tipping point for the temperature

dynamics.

For a given level of carbon concentration M_t, the temperature T_t tends towards an equilibrium that gives radiative balance $T_t \to r^{-1}(g(M_t))$ as $t \to \infty$. Figure 6 shows the equilibria of temperature (solid lines) as a function of carbon concentration when the tipping point is imminent (darkest line), when it is remote (lighter line), and when there is no temperature feedback λ (lightest line). Without temperature feedback λ, the equilibrium temperature is unique and
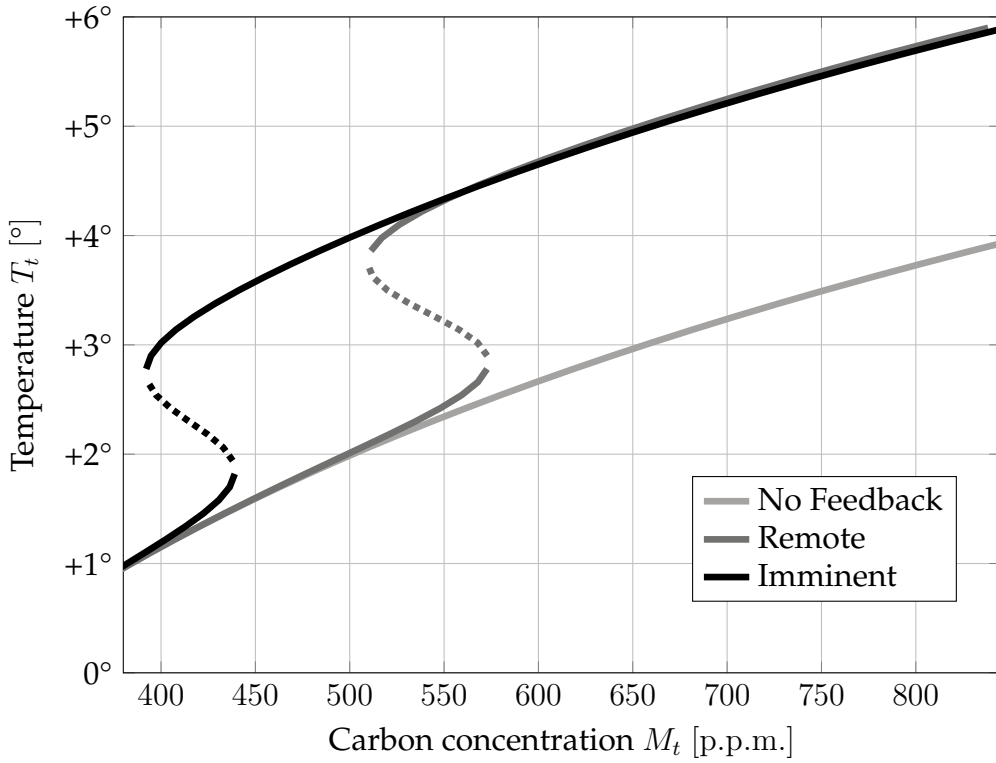

Figure 6: Equilibria of temperature T_t and carbon concentration M_t for an imminent tipping point, a remote tipping point, and no temperature feedback λ. The solid lines show attracting equilibrium and the dashed line repelling equilibrium

it rises with the logarithm of carbon concentration. If a temperature feedback λ is introduced there are two possible temperature regimes: a low temperature regime and a high temperature regime. These coexist for some values of carbon concentration (dashed lines). If the temperature feedback kicks in imminently (imminent scenario), for a carbon concentration M_t between 390 p.p.m. and 440 p.p.m. both a low temperature regime, with $T_t < 1.9°$, and a high temperature regime, with $T_t > 2.9°$ are possible. In the remote scenario this

phenomenon occurs only when carbon concentration M_t is between 510 p.p.m. and 570 p.p.m.. If a planner finds themself in a low temperature regime, the presence of an high temperature regime is hard to detect as it does not affect the relationship between temperature T_t and carbon concentration M_t before the temperature feedback kicks in.[4] If carbon concentration M_t increases and temperature crosses the critical threshold T^c, the old stable and low temperature regime is no longer feasible and only a high stable temperature regime remains. Then, any increase of carbon concentration pushes the system past a tipping point and temperature rapidly converges to the high temperature equilibrium. Crucially, to revert the system back to the lower temperature regime, it is not sufficient to remove just the carbon that caused the system to tip, but it is necessary to remove all carbon until the only stable equilibrium is the low temperature. In Figure 6, this would amount to bring carbon back to $M_t < 390$, when the high temperature regime (solid black line) disappears

We can now ask what path of temperature T_t we would observe in these three scenario if no abatement is implemented and carbon concentration M_t grows at the business-as-usual rate γ_t^b, such that $M_t = M_t^b$. This is illustrated in Figure 7, which shows the median path over 60 years (marked line) of temperatures T_t and carbon concentration M_t under business-as-usual for the model without feedback and the two tipping scenarios, remote and imminent. Each marker is the outcome at the beginning of each decade. The simulations are overlaid onto the equilibria from Figure 6. In case of an imminent tipping point (darkest line) by 2030 the temperature deviates compared to the other scenarios. In case the tipping point is remote, temperature growth cannot be distinguished from a situation without temperature feedback and the two diverge only starting in 2050. In both cases, once the tipping point is crossed and the only regime is the high temperature one, temperature grows quickly to the new equilibrium. After that, the linear relationship between temperature and (log) carbon concentration is restored.

---

[4]Technically, the stable manifold of the model without feedback is a contact element of the stable manifold in the cases with feedback.
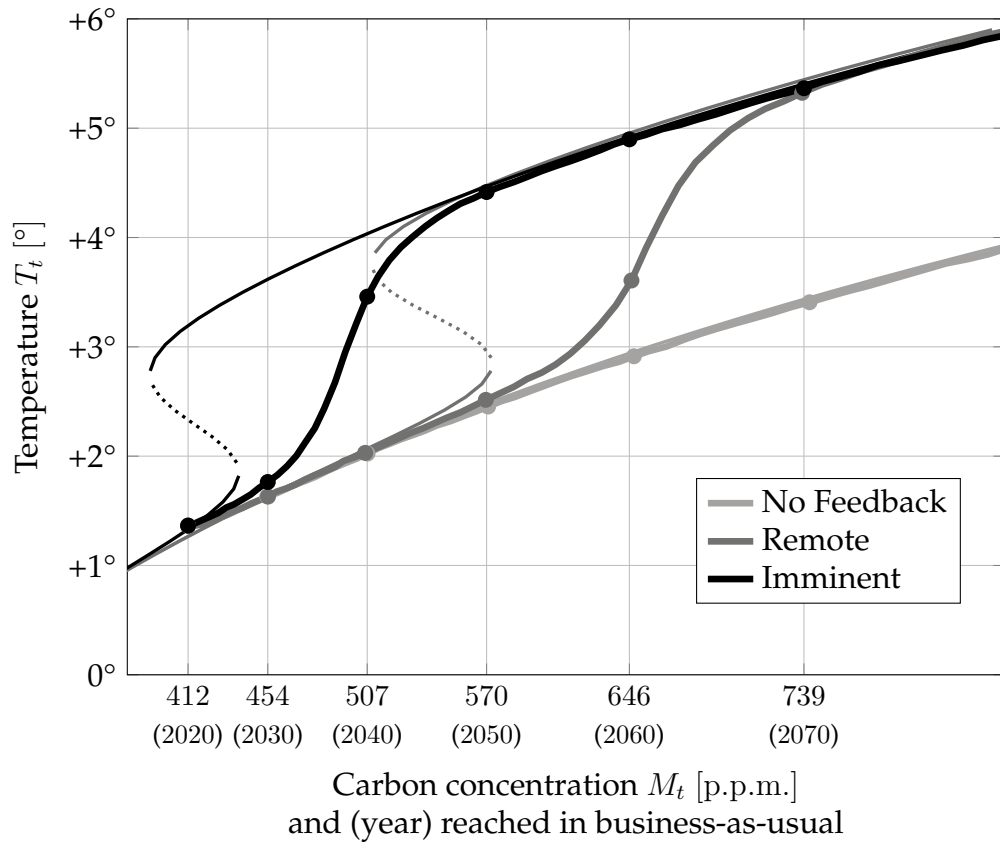
Figure 7: Median of 10000 simulation of temperature T_t and carbon concentration M_t in case of no feedback, an imminent tipping point, and a remote tipping point. Each marker represents the outcome of the median simulation at each decade. The thinner lines represent the equilibrium relationships as in Figure 6.

3.1.4 Irreversable Regime Changes against State-Distribued Catastrophes

Before turning to the economic model, in the following I illustrate why the climate presented here is a more adequate representation of tipping points then the Barro style disasters (Barro, 2009; Pindyck and Wang, 2013) commonly employed in the literature[5]. When modelling a tipping point as a Barro style disaster, one assumes that at each moment in time, with some instantaneous probabilities $\pi(T_t)$ there is a temperature shock of size $q(T_t)$, both of which are increasing in temperature (e.g. Hambel, Kraft and Schwartz 2021; Lemoine and Traeger 2016; Van Der Ploeg and De Zeeuw 2018). Formally, under this assumption, equation (17) of the climate model presented here becomes

$$\epsilon \, dT_t = r_l(T_t) \, dt + g(M_t) \, dt + \sigma_T \, dW_{T,t} + q(T_t) \, dJ_t(T_t) \tag{18}$$

where J_t is a Poisson process with arrival rate $\pi(T_t)$ and r_l, unlike r (15), is linear. For comparison, Figure 8 shows the distribution of temperature generated by the model of this paper (17) and the state-distributed catastrophe model (18), as calibrated in Hambel, Kraft and Schwartz (2021) (see Appendix D for more details on this calibration). Both models capture a key feature of tipping points: as carbon concentration rises, we expect warmer shocks to be more persistent and hence the equilibrium temperature distribution to be skewed (IPCC, 2023; Weitzman, 2014). Yet, the catastrophe model commonly employed in the literature does not display multiple temperature regimes (lower figure). This catastrophe model is hence not suited to answer questions about irreversible tipping points, such as those present in the climate. On the other hand, the model (17) used in this paper (upper figure) generates multiple temperature regimes while still producing a skewed temperature distribution. As discussed in the stylised example in Section 2, a climate with multiple regimes can lead to vastly different optimal abatement paths and costs of tipping.

---

[5]This approach is also known as state-distributed catastrophe (Li, Crépin and Lindahl, 2024)
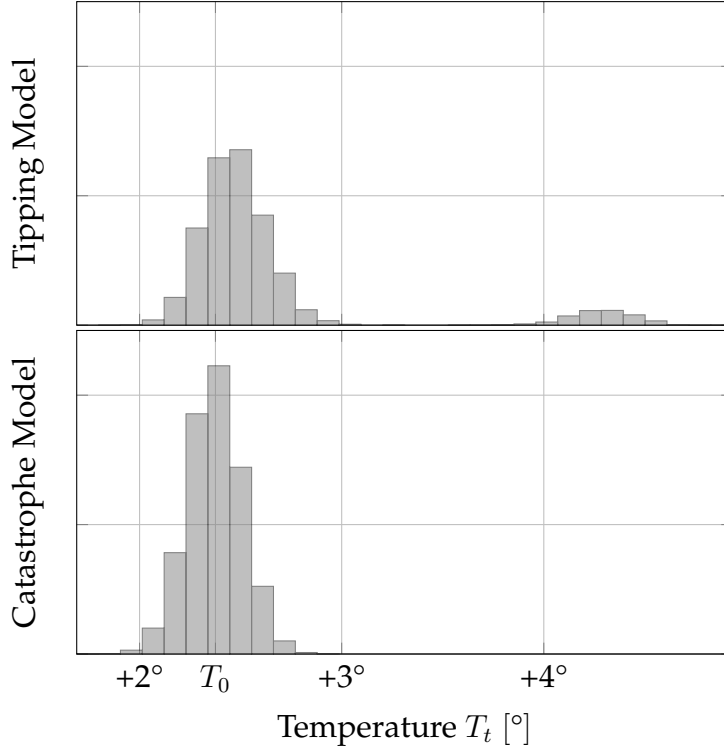
Figure 8: Distribution of temperature T_t obtained from simulation dT_t from (17) (Tipping Model) and (18) (Catastrophe Model) for 1000 years at a constant carbon concentration level $M = 540$ p.p.m. starting at T_0.

3.2 Economy

This section introduces the economy. Following Barro (2009), Pindyck and Wang (2013), and Hambel, Kraft and Schwartz (2021), this is modelled as an Harrod-Domar economy.

3.2.1 Capital Accumulation and Climate Damages

Output

$$Y_t = A_t K_t. \tag{19}$$

is the product of the capital stock K_t and its productivity A_t. The latter grows at a constant rate ϱ. Output Y_t can be used for investment in capital I_t, abatement expenditures B_t, or consumption C_t. This implies the nominal budget constraint

$$Y_t = I_t + B_t + C_t. \tag{20}$$

Capital K_t depreciates at a rate δ_k but can be substituted by capital investments I_t, which incurs, along with abatement expenditure B_t, in quadratic adjustment costs

$$\frac{\kappa}{2} \left(\frac{I_t + B_t}{K_t} \right)^2 K_t. \tag{21}$$

Climate change interacts with the economy by lowering capital growth via damages $d(T_t)$ which are increasing in temperature T_t. Following Weitzman (2012), I assume the damage function to take the form

$$d(T_t) := \xi \, T_t^v. \tag{22}$$

The calibrated damage function is displayed in Figure 9. This stylised form cap-

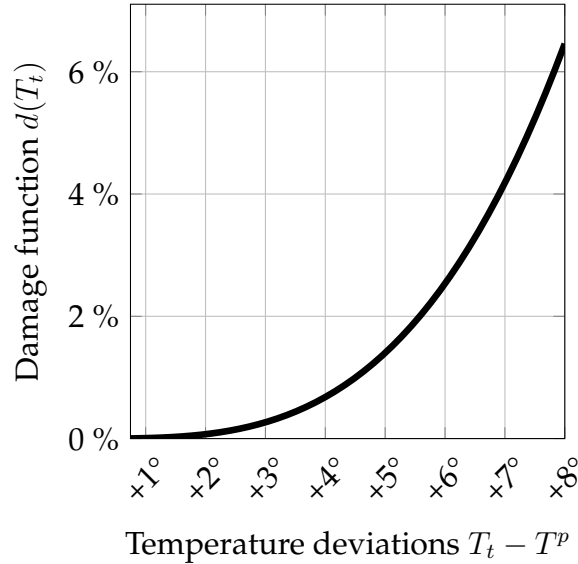**Figure 9:** Damage function with the Weitzman (2012) calibration.

tures the empirical evidence that under higher temperature levels some forms of capital, particularly in the agricultural (Dietz and Lanz, 2019) or manufacturing sectors (Dell, Jones and Olken, 2009, 2012), become more expensive or harder to substitute. A common alternative in the literature is to assume that higher temperatures wipe out part of the capital stocks (Nordhaus, 1992). A thorough comparison of these two assumptions can be found in Hambel, Kraft and Schwartz (2021).

Combining the endogenous growth of capital and the climate damages, the

growth rate of capital satisfies

$$\frac{\mathrm{d}K_t}{K_t} = \left(\frac{I_t}{K_t} - \delta_k - \frac{\kappa}{2} \left(\frac{I_t + B_t}{K_t} \right)^2 \right) \mathrm{d}t - d(T_t)\,\mathrm{d}t + \sigma_k\,\mathrm{d}W_{k,t}, \qquad (23)$$

where $W_{k,t}$ is a Wiener process.

In the following, I link the abatement costs B_t with the abatement rate α_t, introduced in the previous section. Introduce $\beta_t \coloneqq B_t/Y_t$ the fraction of output devoted to abatement. I assume this to be a quadratic function of the fraction of abated emissions $\varepsilon(\alpha_t)$ (11), namely,

$$\beta_t(\varepsilon(\alpha_t)) = \frac{\omega_t}{2}\,\varepsilon(\alpha_t)^2. \qquad (24)$$

Under this assumption, no abatement is free, as $\beta_t(0) = 0$. At a fixed time t, a higher abatement rate α_t and hence a higher emission reduction $\varepsilon(\alpha_t)$ vis-à-vis the business-as-usual scenario, becomes increasingly costly at linear rate $\omega_t \varepsilon(\alpha_t)$. It is common in the literature to assume the marginal abatement costs to be proportional to output and linear in abatement efforts (Baker, Clarke and Shittu, 2008; Dietz and Venmans, 2019; Nordhaus, 1992, 2017). As noted by Dietz and Venmans (2019, p.112-113), the proportionality with output arises because higher output growth increases energy demand. This must be satisfied with low-carbon energy technology which display decreasing marginal productivity. The linearity in abatement efforts is assumed as it matches the empirical estimates provided in the IPCC Fifth Assessment Report (2023).

As time progresses, so does abatement technology and a given abatement objective becomes cheaper, as a fraction of output. This is modelled by letting the exogenous technological parameter ω_t decrease exponentially over time

$$\omega_t = \omega_0 e^{-\omega_r t}. \qquad (25)$$

Following (Nordhaus, 2017), I assume that full abatement $\varepsilon(\alpha_t) = 1$ costs 11% of GDP in 2020 and 2.7% of GDP in 2100. These estimates are in line with a large

literature estimating marginal abatement curves (see the meta-analysis by Kuik, Brander and Tol, 2009). The resulting marginal abatement curves are displayed in Figure 10.
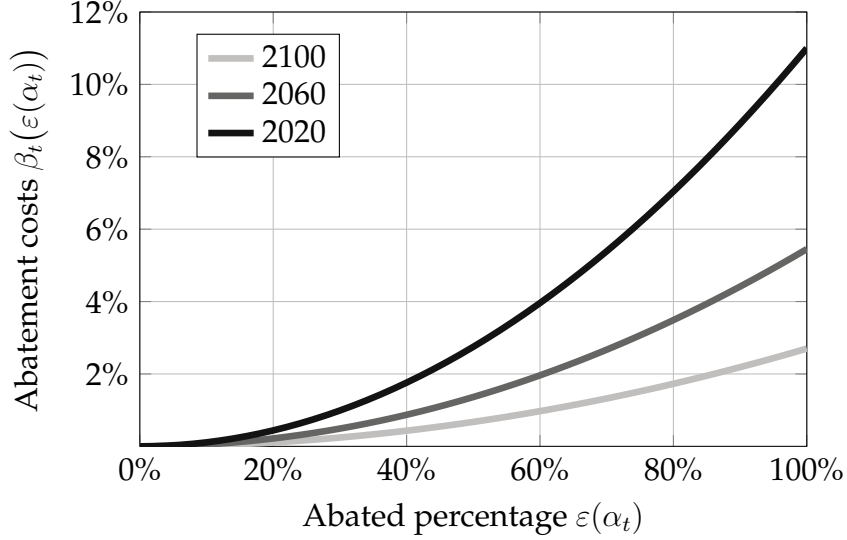

Figure 10: Calibrated marginal abatement curves $\beta_t'(\varepsilon) = \omega_t \varepsilon$ at different times t.

Finally, let

$$\chi_t := \frac{C_t}{Y_t} \tag{26}$$

be the fraction of output devoted to consumption. Using the budget constraint (20) and the two controlled rates, the abatement efforts α_t and the consumption rate χ_t, the growth rate of capital (23) can be rewritten, in terms of growth rates, as

$$\frac{\mathrm{d}K_t}{K_t} = \Big(\underbrace{\phi_t(\chi_t)}_{\text{growth}} - \overbrace{A_t \beta_t(\varepsilon(\alpha_t))}^{\text{abatement}} - \underbrace{d(T_t)}_{\text{climate}} \Big) \, \mathrm{d}t + \sigma_k \, \mathrm{d}W_{k,t} \tag{27}$$

where

$$\phi_t(\chi_t) := A_t(1 - \chi_t) - \frac{\kappa}{2} A_t^2 (1 - \chi_t)^2 - \delta_k \tag{28}$$

is an endogenous growth component, $\beta_t(\varepsilon(\alpha_t))$ is the fraction of output allocated to abatement for an abatement rate α_t, and $d(T_t)$ are the damages from climate change. This formulation makes the trade-off between climate abatement and economic growth apparent. Devoting fewer resources to abatement to pursue higher capital growth, and hence, output growth, yields higher future

23

temperature and can put the economy in a lower growth path altogether.

Finally, as output Y_t is the product of capital K_t and productivity A_t, its growth rate differs from that of capital by the growth rate of productivity

$$\frac{\mathrm{d}Y_t}{Y_t} = \varrho + \frac{\mathrm{d}K_t}{K_t}. \tag{29}$$

4 Optimal Abatement

Given the climate and economic dynamics described in the previous section, I introduce the objective of the social planner and the resulting optimal policies. At time t given the state of temperature, carbon concentration, carbon in sinks, and output $X_t := (T_t, M_t, N_t, Y_t)$, societal utility is recursively defined as

$$V_t(X_t) = \sup_{\chi, \alpha} \mathbb{E}_t \int_t^\infty f(\chi_s(X_s)Y_s, V_s(X_s)) \, \mathrm{d}s \tag{30}$$

where χ and α are continuous policies over time and the state space, and f is the Epstein-Zin aggregator

$$f(C, V) := \rho \frac{(1-\theta) V}{1 - 1/\psi} \left(\left(\frac{C}{((1-\theta)V)^{\frac{1}{1-\theta}}} \right)^{1-1/\psi} - 1 \right). \tag{31}$$

Consumption is integrated into a utility index by means of the Epstein-Zin integrator (Duffie and Epstein, 1992). This aggregator plays a dual role. First, it disentangles the role of relative risk aversion θ, elasticity of intertemporal substitution ψ, and the discount rate ρ in determining optimal abatement paths. Second, it circumvents the known paradoxical result that abatement policies becomes less ambitious as society becomes more risk averse Pindyck and Wang (2013). As in Hambel, Kraft and Schwartz (2021), the model presented here assumes $\rho = 1.5\%$, $\theta = 10$ and $\psi = 0.75$. For a more detailed discussion on the calibration of these parameters see Pindyck and Wang (2013, Section 2) and for their role in determining optimal abatement see Hambel, Kraft and Schwartz (2021). Details on the numerical solution of problem (30) are given in Appendix

A.

As mentioned above, we consider two possible dynamics for temperature T_t: one with an imminent and one with a remote tipping point. Let $\underline{\alpha}_t$ and $\overline{\alpha}_t$ be the optimal abatement in case of an imminent and a remote tipping point respectively. Figure 11 shows the resulting optimal policies. Each panel shows the fraction $\varepsilon_t \coloneqq \varepsilon(\alpha_t)$ of abated emissions compared to the business-as-usual as a function of the current carbon concentration M_t, in the imminent (left) and remote (right) tipping point. As the tipping point generates multiple tempera-
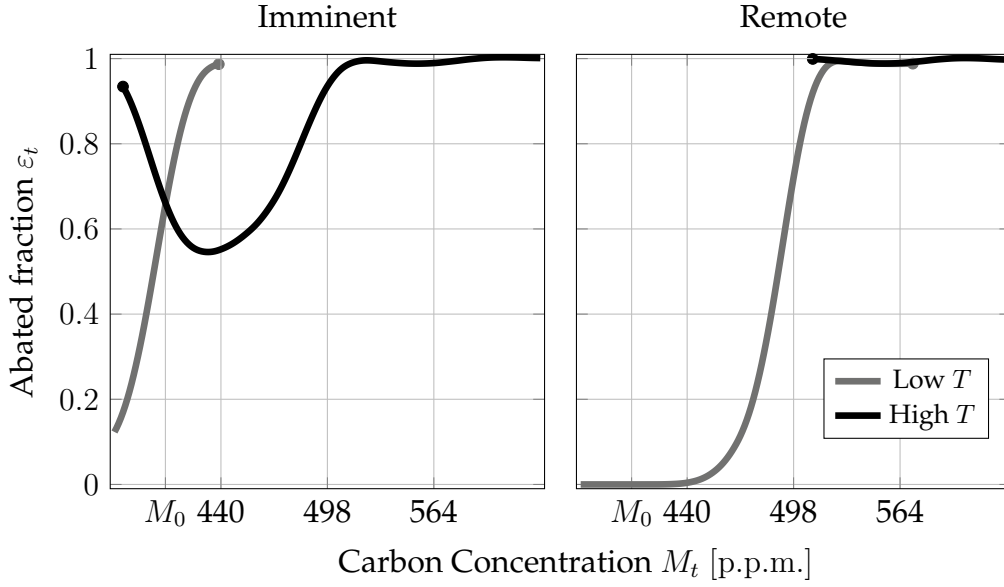

Figure 11: Fraction of abated emissions ε_t at different levels of carbon concentration M_t, for an imminent (left panel) and remote (right panel) point. To aid illustration, all other dimensions (T_t, N_t, Y_t) are set to their equilibrium value. As for some values of M_t there are two equilibria of temperature T_t, two curves are shown. The current level of carbon concentration is indicated with M_0.

ture regimes for a given carbon concentration level M_t, each panel shows two curves. The lighter curve represents the optimal abatement before tipping, in a low temperature regime. The darker curve represents the optimal abatement after tipping, in a high temperature regime. The optimal policy is hence not unique and switches in the event of tipping. In case of an imminent tipping point (left panel) before having tipped (lighter curve), the fraction of abated emission ε_t increases rapidly to 1 as carbon concentration rises. If the tipping point is crossed and the climate system switches to a high temperature regime

abatement efforts are scaled back (darker curve) as the climate is irreversibly in a regime of high temperature. This results underpins a strong policy result: crossing a tipping point immediately weakens abatement incentives, hence, it is optimal to rapidly scale up abatement before that happens. This aspect of optimal abatement policies with tipping points cannot be captured by the social cost of carbon, since the marginal benefit of abating jumps down once the climate has tipped. Finally, notice that, if the climate has tipped but carbon concentration is low, it is still worth abating a large fraction of emissions (dark curve is u-shaped). The incentive to remain at a low carbon concentration is that a random negative shock in temperature can push the system back to a low-temperature regime. Once the carbon concentration has increased, this becomes increasingly rare and it is hence not worth abating on the off chance it would happen. At the other extreme, if the tipping point is remote (right panel) it does not affect optimal policy. Abatement efforts are increasing in carbon concentration and full abatement is reached, in both regimes, at around 500 p.p.m.. In this case, direct climate damages are sufficiently large to warrant reaching net-zero before there is any risk of crossing the tipping point.

These policies, when implemented, yield a path of temperature and, as a consequence, temperature damages. Figure 12 shows the median path of the fraction ε_t of abated emission (solid line) and the resulting temperature path T_t with 95% simulation intervals (dotted lines), for an imminent (left panel) and a remote (right panel) tipping point.
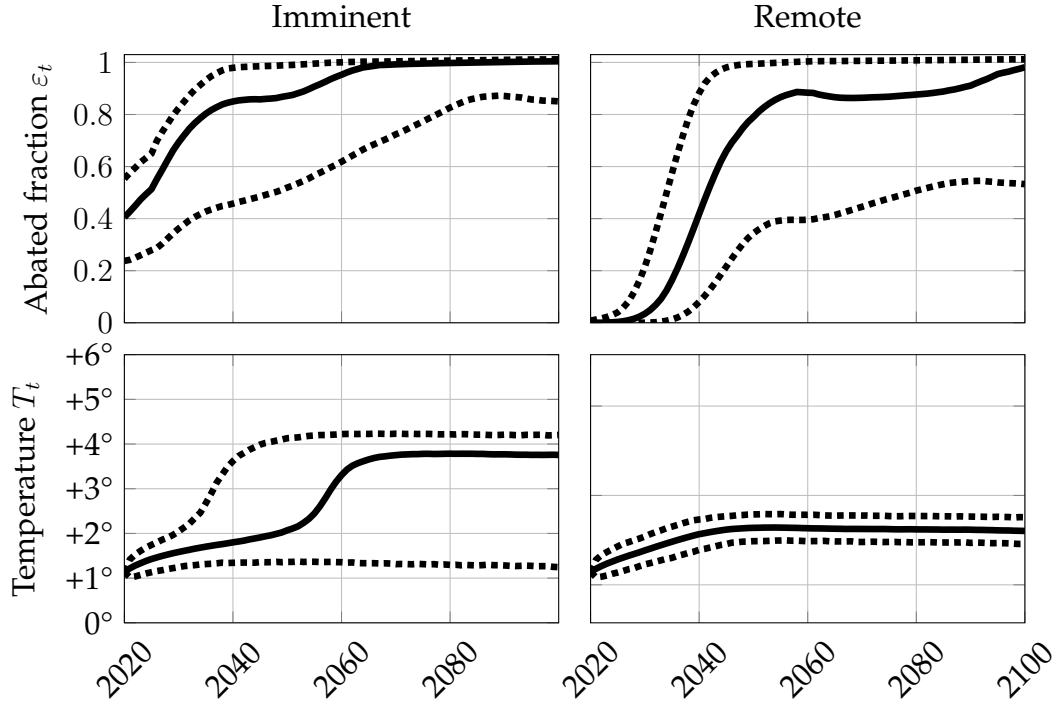
Figure 12: Median (solid line) and 95% simulation intervals (dotted line) of abated fraction ε_t and temperature T_t under optimal policies in the imminent and remote scenarios. 10000 simulations.

When the tipping point is imminent, optimal abatement is promptly ramped up. In the median case 40 % of the business-as-usual emissions are abated immediately. Thereafter, abatement ramps up and net-zero is attained by 2060. These large efforts are not sufficient to completely prevent tipping as by 2040 the climate system has tipped with 5% probability and by 2060 with 50% probability. In case the tipping point is remote, the planner has more time to postpone abatement, which is cheaper in the future, and is able to stabilise temperature at around $2°$ without tipping. When choosing abatement policies, the planners are balancing two sources of societal costs: abatement expenditures $\beta_t(\epsilon_t)$ and their adjustment costs against climate damages $d(T_t)$. Figure 13 shows the average costs in each decade, as a fraction of output Y_t, in the median scenario, broken down into these three cost sources.
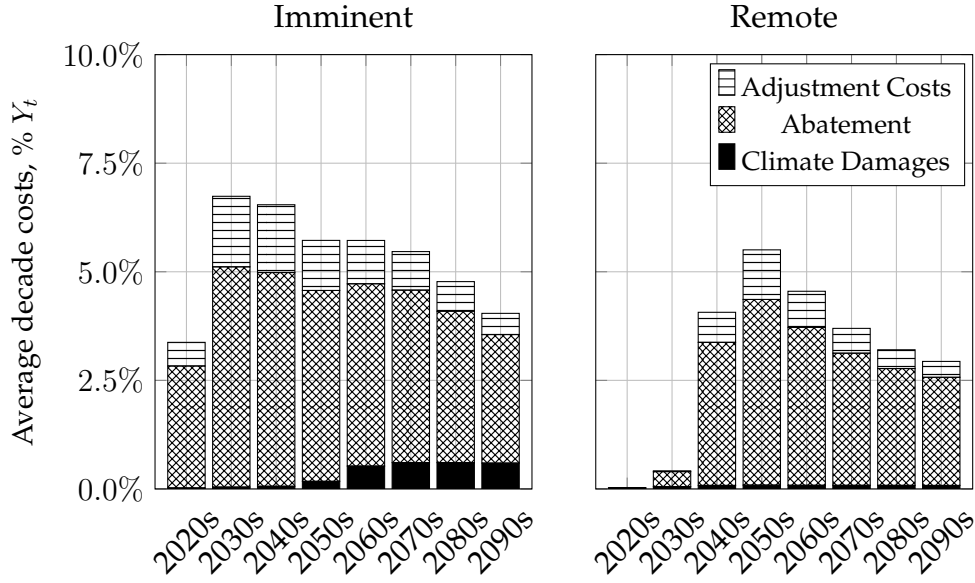
27

Figure 13: Costs in the median scenario as a fraction of output Y_t, broken down in adjustment costs, abatement and climate damages.

If the tipping point is imminent (left panel), optimal abatement costs quickly build up over the next two decades to around 5% of output before stabilising at 4% of output. Because abatement occurs quickly, society incurs in large adjustment costs of up to 2% of output, which are then absorbed over time. Despite these efforts, climate damages stabilise at around 1% of output. In case of a remote tipping point, the planner can scale abatement expenditures more slowly, thereby incurring in moderate adjustment costs and benefiting from improved technology. In both cases, the cost of the abatement required to stabilise the climate shrinks thanks to technological improvement ω_t (25), while climate damages are persistent as tipping points are irreversible.

The costs do not give the full picture, as the planner has preferences over consumption, given by the Epstein-Zin aggregator (31). To give estimates on the costs of tipping points under optimal policies, one needs to focus on the net present values, which satisfy the maximisation (30) at time $t = 0$. Denote the net present value by $\overline{V}_0$, when the tipping point is remote, and $\underline{V}_0$, when the tipping point is imminent. These two values can be translated into dollars by computing the corresponding certainty equivalent, that is the amount of constant and certain yearly output that yields the same net present value (more details on

28

the calculation are given in Appendix B). This quantity internalises all future climate damages and output growth, and their respective uncertainties. In case of a remote tipping point, the certainty equivalent $\overline{CE}$ is 54.83 trillionUS\$/year (72.33% current output), while in case of an imminent tipping point, the certainty equivalent $\underline{CE}$ is 52.95 trillionUS\$/year (69.86% current output). First, both certainty equivalents are significantly lower than current output Y_0. The gap can be attributed to societal risk aversion: society is willing to give up almost 30% of output to perfectly smooth income shocks. Second, the cost of the temperature feedback being triggered imminently, at $T^c = 1.5°$, rather than remotely, $T^c = 2.5°$, is 1.87 trillionUS\$/year or 2.47% of current output. This quantity shows how costly procrastination can be.

5   The Cost of Tipping Point Uncertainty

The previous section discussed the optimal policies of a planner that knows whether the tipping point is imminent or remote. Yet, tipping points are unpredictable. This section gives an upper bound on the cost of this unpredictability. To do so, I consider two extreme scenario. First, I consider a *wishful thinker* planner, denoted w, who erroneously assumes the tipping point to be remote, while it is in fact imminent. Once the temperature feedback kicks in, the planner detects the tipping point and switches to the optimal abatement strategy. In other words, letting

$$\tau := \inf_t \{T_t \geq T^c\} \tag{32}$$

be the time at which the feedback effects kick-in, the abatement strategy employed by w is given by

$$\alpha_t^w := \begin{cases} \overline{\alpha}_t & \text{if } t < \tau, \\ \underline{\alpha}_t & \text{if } t \geq \tau. \end{cases} \tag{33}$$

Second, I consider a *prudent* planner, denoted p, who erroneously assumes the tipping point to be imminent, while it is in fact remote. Again, in case the feedback loop is triggered, the planner switches to the optimal strategy, such

that

$$
\alpha_t^p := \begin{cases} \underline{\alpha}_t & \text{if } t < \tau, \\ \overline{\alpha}_t & \text{if } t \geq \tau. \end{cases} \tag{34}
$$

Table 1 summarises the possible tipping points and the strategies employed before the temperature feedback is triggered, $t < \tau$.

		Tipping Point	
		Imminent	Remote
Policies	$\underline{\alpha}$	Optimal	Prudent p
	$\overline{\alpha}$	Wishful thinker w	Optimal

Table 1: Strategies used before tipping $t < \tau$ for the four scenarios. After tipping $t \geq \tau$ optimal strategies are used in all scenarios.

The wishful thinker planner w incurs in the maximal climate damages. The prudent planner p incurs in the maximal abatement and adjustment costs. Hence, the costlier of the two sub-optimal strategies is an upper bound to the cost of the tipping point.

Focusing first on the wishful thinker w, Figure 14 shows the path of the abated fraction of emissions ε_t (left panel) and the resulting temperature T_t (right panel) whenever α^w (33) is used in face of an imminent tipping point.

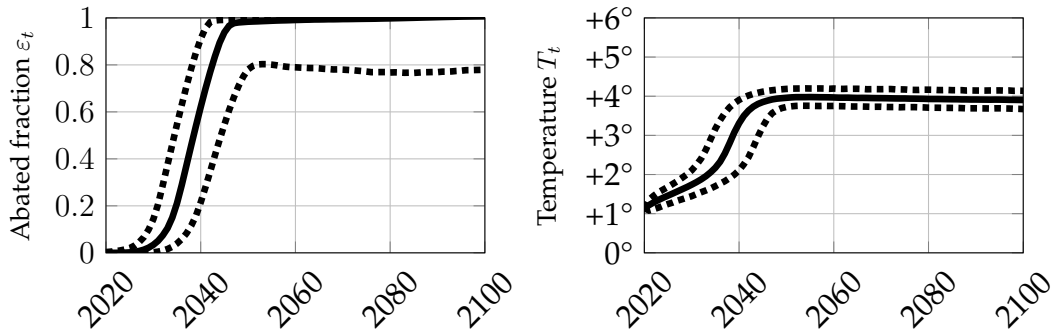**Figure 14:** Median and 95% simulation intervals of the abated fraction of emissions ε_t (left panel) and the resulting the temperature T_t (right panel). Calculated from 10000 simulations using policy (33)

In the first decade, the planner erroneously believes the tipping point to be remote, and hence postpones abatement efforts, as the median $\varepsilon_t \approx 0$ for $t <$

2030. Once the temperature feedback kicks in, the planner "slams the break" and quickly ramps up abatement, achieving net-zero in the 2040s, in most cases. Despite the quick abatement ramp-up, by 2050 the climate has tipped and is hence in a high temperature regime with 95% probability. When compared to the optimal abatement path under an imminent tipping point (left column of Figure 12), the abatement path path w clearly incurs in much larger climate damages, as the climate tips sooner and with large probability, and in larger adjustment costs, as abatement measures need to be ramped up more quickly. Figure 15 shows a breakdown of the cost incurred by the wishful thinker w.

Figure 15: Costs in the median scenario of a wishful thinker w planner as a fraction of output Y_t, broken down in adjustment costs, abatement and climate damages.

In the first two decades, the planner implements little abatement. Yet, in the 2040s as the temperature feedback kicks in, abatement expenditures ramp up quickly. Rapidly ramping up abatement incurs in large adjustment costs, which peak at more than 3% of output. This delay in abatement is not sufficient to prevent tipping, which brings about large and, most importantly irreversible, climate damages of around 1% of output. This scenario gives an upper bound on the possible climate damages society can incur if it delays optimal abatement until after the feedback kicks in.

I then do an analogous experiment for the prudent planner p. Figure 16 dis-

plays the path of the abated fraction of emissions ε_t (left panel) and temperature T_t (right panel) resulting from abatement α^p (34) whenever the tipping point is remote.
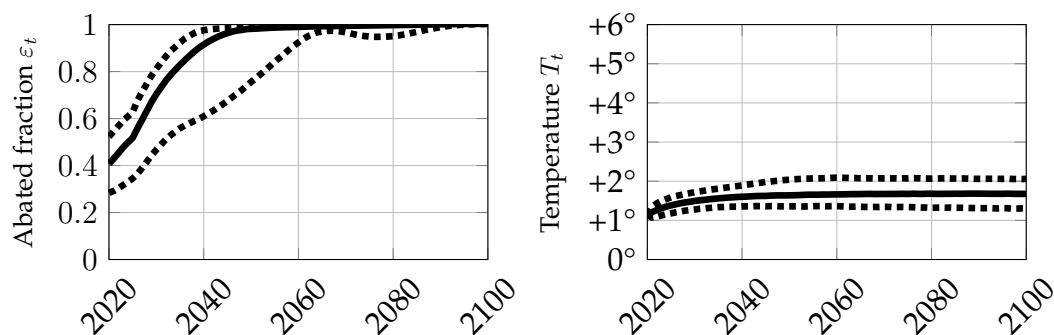
Figure 16: Median and 95% simulation intervals of the abated fraction of emissions ε_t (left panel) and the resulting the temperature T_t (right panel). Calculated from 10000 simulations using policy (34)

The prudent planner fully abates emissions already be the early 2040s and quickly stabilises temperature at around $2.5°$. Figure 17 breaks down the cost incurred by the prudent p planner.

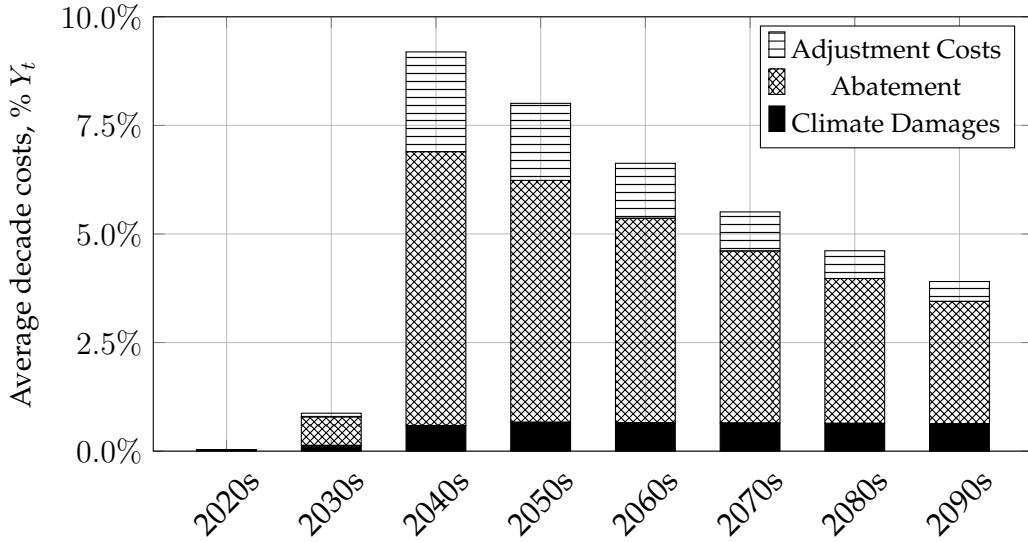**Figure 17:** Costs in the median scenario of a prudent p planner as a fraction of output Y_t, broken down in adjustment costs, abatement and climate damages.

The prudent planner sustains abatement costs of around or more than 6% of output between 2030 and 2070. This fast and aggressive abatement schedule accumulates large adjustment costs that can be as large as 2% of output. In

return, the climate damages are kept below 0.1% of output. This scenario gives an upper bound on the abatement costs society can incur in if it abates quickly assuming a tipping point is imminent.
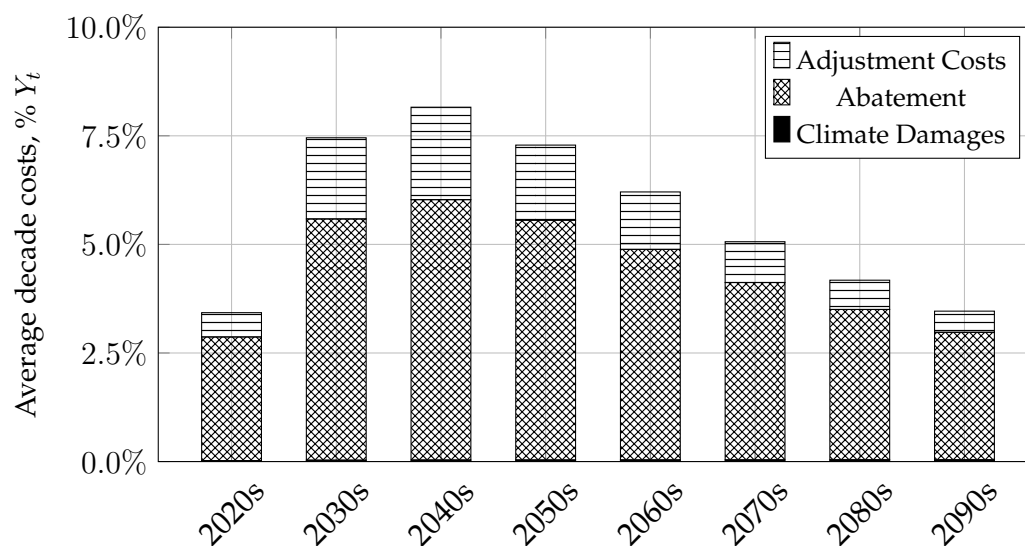
The breakdowns presented here (Figures 15 and 17) give upper bounds on the climate damages (w) and abatement cost (p). These are just nominal costs, that do reflect climate and economic risk and do not internalise societal preference. Hence, as in the optimal scenario presented in the previous section, I compute certainty equivalents CE^w and CE^p, in trillionUS\$/year, for the wishful thinker and prudent case respectively (more detail on how they are computed is given in Appendix B). These are summarised in Table 2.

	Tipping Point	
	Imminent	Remote
$\underline{\alpha}$	$\underline{CE} = 52.95\text{trUS\$/y } (69.86\%Y_0)$	$CE^p = 29.92\text{trUS\$/y } (39.48\%Y_0)$
$\overline{\alpha}$	$CE^w = 26.7\text{trUS\$/y } (35.23\%Y_0)$	$\overline{CE} = 54.83\text{trUS\$/y } (72.33\%Y_0)$

Table 2: Certainty equivalents for the four scenarios in trillionUS\$/year. In brackets, the certainty equivalent is expressed as a percentage of current output Y_0.

The Table has the same structure as Table 1. Each cell contains the certainty equivalent of the corresponding scenario, in trillionUS\$/year and as a percentage of current output Y_0. These quantities allow to bound the cost of the tipping point. On the one hand, a prudent strategy p incurs in suboptimal abatement and adjustment costs. These are $\overline{CE} - CE^p = 24.9$ trillionUS\$/year or 32.86% of current output. On the other hand, a wishful thinker strategy w incurs large and permanent climate damages. This can have costs up to $\underline{CE} - CE^w = 26.25$ trillionUS\$/year or 34.63% of current output. Notice that, albeit costly, a prudent strategy p can be up to $CE^p - CE^w = 3.22$ trillionUS\$/year or 4.56% of current output cheaper than a wishful thinker strategy w.

The cost of uncertainty of tipping points, which results in the inability of society to implement optimal strategies, can be as large as 26.25 trillionUS\$/year, which is more than a third of current world output. These large costs reflect the crucial role tipping points play when trying to deal with climate change: if they

can be foreseen they are easily avoided; if they are ignored they can be catastrophic. Second, in the face of uncertainty, it is 3.22 trillionUS\$/year cheaper to tread carefully, as prudence, however costly, is more effective then wishful thinking.

6   Discussion

This paper estimates the economic cost of uncertain and irreversible climate tipping points. A temperature feedback is integrated in a state-of-the-art integrated assessment model, which is then calibrated. To avoid attaching a prior distribution on the horizon of a tipping point, I consider two limit scenarios, among those consistent with the climate literature: that of an *imminent* and a *remote* tipping point. Using these two scenarios, I first compute an upper bound on cost of tipping points and then estimate the value of a prudent strategy in face of uncertainty, compared to a wishful thinking strategy postponing abatement until the tipping point is identified.

The cost of an uncertain and irreversible tipping point can be as high as 32% of current world output. This estimate is much larger than the cost of tipping points found in the economic literature, despite having comparable calibrations (e.g. Lemoine and Traeger, 2016 or Van Der Ploeg and De Zeeuw, 2018). The are two reasons for this gap. The first reason is that this estimate is an upper bound on the cost, while most estimates given in the literature are median costs. On the one hand, this is reassuring: the real cost of tipping points surely will fall below 32% of current world output. On the other hand, it suggests that under more pessimistic priors on the tipping point, which cannot be ruled out given the current uncertainty on temperature feedback, these median estimates can grow substantially. The second reason for such an estimate gap is that the climate economic literature has, in large part, modelled tipping points as large yet transient increases in temperature. This is unrealistic for most tipping points which are expected to introduce uncertain yet irreversible temperature regime shifts.

These results suggest that policy can be lead astray by measures of marginal benefits and costs, such as the social cost of carbon. In a climate that can experience irreversible changes, if there is some uncertainty on when these might happen, these measures are not well defined. When facing this uncertainty, a prudent strategy which abates emissions quickly is very costly but much cheaper than delaying abatement with the risk of tipping the climate.

References

Ackerman, Frank, Elizabeth A. Stanton, and Ramón Bueno. 2013. "Epstein–Zin Utility in DICE: Is Risk Aversion Irrelevant to Climate Policy?" *Environmental and Resource Economics*, 56(1): 73–84. 48

Armstrong McKay, David I., Arie Staal, Jesse F. Abrams, Ricarda Winkelmann, Boris Sakschewski, Sina Loriani, Ingo Fetzer, Sarah E. Cornell, Johan Rockström, and Timothy M. Lenton. 2022. "Exceeding 1.5°C Global Warming Could Trigger Multiple Climate Tipping Points." *Science*, 377(6611): eabn7950. 2, 5, 14

Ashwin, Peter, Sebastian Wieczorek, Renato Vitolo, and Peter Cox. 2012. "Tipping Points in Open Systems: Bifurcation, Noise-Induced and Rate-Dependent Examples in the Climate System." *Philosophical Transactions of the Royal Society A: Mathematical, Physical and Engineering Sciences*, 370(1962): 1166–1184. 13

Baker, Erin, Leon Clarke, and Ekundayo Shittu. 2008. "Technical Change and the Marginal Cost of Abatement." *Energy Economics*, 30(6): 2799–2816. 22

Barro, Robert J. 2009. "Rare Disasters, Asset Prices, and Welfare Costs." *American Economic Review*, 99(1): 243–264. 4, 19, 20

Ben-Yami, Maya, Andreas Morr, Sebastian Bathiany, and Niklas Boers. 2024. "Uncertainties Too Large to Predict Tipping Times of Major Earth System Components from Historical Data." *Science Advances*, 10(31): eadl4841. 2, 9, 14

Bierkens, Joris, Paul Fearnhead, and Gareth Roberts. 2019. "The Zig-Zag Process and Super-Efficient Sampling for Bayesian Analysis of Big Data." *The Annals of Statistics*, 47(3). 5, 47

Boulton, Chris A., Lesley C. Allison, and Timothy M. Lenton. 2014. "Early Warning Signals of Atlantic Meridional Overturning Circulation Collapse in a Fully Coupled Climate Model." *Nature Communications*, 5(1): 5752–5752. 14

Cai, Yongyang, Timothy M. Lenton, and Thomas S. Lontzek. 2016. "Risk of Multiple Interacting Tipping Points Should Encourage Rapid CO2 Emission Reduction." *Nature Climate Change*, 6(5): 520–525. 4

Crost, Benjamin, and Christian P. Traeger. 2013. "Optimal Climate Policy: Uncertainty versus Monte Carlo." *Economics Letters*, 120(3): 552–558. 48

Dell, Melissa, Benjamin F Jones, and Benjamin A Olken. 2009. "Temperature and Income: Reconciling New Cross-Sectional and Panel Estimates." *American Economic Review*, 99(2): 198–204. 21

Dell, Melissa, Benjamin F Jones, and Benjamin A Olken. 2012. "Temperature Shocks and Economic Growth: Evidence from the Last Half Century." *American Economic Journal: Macroeconomics*, 4(3): 66–95. 21

Dietz, Simon, and Bruno Lanz. 2019. "Growth and Adaptation to Climate Change in the Long Run." IRENE Institute of Economic Research IRENE Working Papers 19-09. 21

Dietz, Simon, and Frank Venmans. 2019. "Cumulative Carbon Emissions and Economic Policy: In Search of General Principles." *Journal of Environmental Economics and Management*, 96: 108–129. 22

Dietz, Simon, Frederick Van Der Ploeg, Armon Rezai, and Frank Venmans. 2020. "Are Economists Getting Climate Dynamics Right and Does It Matter?" *SSRN Electronic Journal*. 4

Ditlevsen, Peter D., and Sigfus J. Johnsen. 2010. "Tipping Points: Early Warning and Wishful Thinking." *Geophysical Research Letters*, 37(19): 2010GL044486. 14

Duffie, Darrell, and Larry G. Epstein. 1992. "Asset Pricing with Stochastic Differential Utility." *Review of Financial Studies*, 5(3): 411–436. 24

Epstein, Larry G., and Stanley E. Zin. 1989. "Substitution, Risk Aversion, and the Temporal Behavior of Consumption and Asset Returns: A Theoretical Framework." *Econometrica*, 57(4): 937. 46

Ghil, Michael, and Stephen Childress. 2012. *Topics in Geophysical Fluid Dynamics: Atmospheric Dynamics, Dynamo Theory, and Climate Dynamics.* Vol. 60, Springer Science & Business Media. 13

Greiner, Alfred, and Willi Semmler. 2005. "Economic Growth and Global Warming: A Model of Multiple Equilibria and Thresholds." *Journal of Economic Behavior & Organization*, 57(4): 430–447. 5

Hambel, Christoph, Holger Kraft, and Eduardo Schwartz. 2021. "Optimal Carbon Abatement in a Stochastic Equilibrium Model with Climate Change." *European Economic Review*, 132: 103642. 4, 19, 20, 21, 24, 43, 48, 50, 51

IPCC. 2023. *Climate Change 2021 – The Physical Science Basis: Working Group I Contribution to the Sixth Assessment Report of the Intergovernmental Panel on Climate Change.* . 1 ed., Cambridge University Press. 14, 19, 22

Kamien, Morton I., and Nancy L. Schwartz. 1971. "Sufficient Conditions in Optimal Control Theory." *Journal of Economic Theory*, 3(2): 207–214. 4

Kriegler, Elmar, Nico Bauer, Alexander Popp, Florian Humpenöder, Marian Leimbach, Jessica Strefler, Lavinia Baumstark, Benjamin Leon Bodirsky, Jérôme Hilaire, David Klein, Ioanna Mouratiadou, Isabelle Weindl, Christoph Bertram, Jan-Philipp Dietrich, Gunnar Luderer, Michaja Pehl, Robert Pietzcker, Franziska Piontek, Hermann Lotze-Campen, Anne Biewald, Markus Bonsch, Anastasis Giannousakis, Ulrich Kreidenweis, Christoph Müller, Susanne Rolinski, Anselm Schultes, Jana Schwanitz, Miodrag Stevanovic, Katherine Calvin, Johannes Emmerling, Shinichiro Fujimori, and Ottmar Edenhofer. 2017. "Fossil-Fueled Development (SSP5):

An Energy and Resource Intensive Scenario for the 21st Century." *Global Environmental Change*, 42: 297–315. 11, 12

Kuik, Onno, Luke Brander, and Richard S.J. Tol. 2009. "Marginal Abatement Costs of Greenhouse Gas Emissions: A Meta-Analysis." *Energy Policy*, 37(4): 1395–1403. 23

Kushner, Harold J., and Paul Dupuis. 2001. *Numerical Methods for Stochastic Control Problems in Continuous Time.* Vol. 24 of *Stochastic Modelling and Applied Probability*, New York, NY:Springer New York. 5, 45, 46

Lemoine, Derek, and Christian P. Traeger. 2016. "Ambiguous Tipping Points." *Journal of Economic Behavior & Organization*, 132: 5–18. 4, 19, 34

Lemoine, Derek, and Christian Traeger. 2014. "Watch Your Step: Optimal Policy in a Tipping Climate." *American Economic Journal: Economic Policy*, 6(1): 137–166. 4

Le Quéré, Corinne, Christian Rödenbeck, Erik T. Buitenhuis, Thomas J. Conway, Ray Langenfelds, Antony Gomez, Casper Labuschagne, Michel Ramonet, Takakiyo Nakazawa, Nicolas Metzl, Nathan Gillett, and Martin Heimann. 2007. "Saturation of the Southern Ocean CO2 Sink Due to Recent Climate Change." *Science*, 316(5832): 1735–1738. 11

Li, Chuan-Zhong, Anne-Sophie Crépin, and Therese Lindahl. 2024. "The Economics of Tipping Points: Some Recent Modeling and Experimental Advances." *International Review of Environmental and Resource Economics*, 18(4): 385–442. 4, 19

Lin, Xu, and Sweder van Wijnbergen. 2023. "The Social Cost of Carbon under Climate Volatility Risk." Tinbergen Institute Tinbergen Institute Discussion Papers 23-032/IV. 4

Lontzek, Thomas S., Yongyang Cai, Kenneth L. Judd, and Timothy M. Lenton. 2015. "Stochastic Integrated Assessment of Climate Tipping Points

Indicates the Need for Strict Climate Policy." *Nature Climate Change*, 5(5): 441–444. 4, 48

Mäler, Karl-Göran, Anastasios Xepapadeas, and Aart de Zeeuw. 2003. "The Economics of Shallow Lakes." *Environmental and Resource Economics*, 26(4): 603–624. 5

McGuffie, Kendal, and Ann Henderson-Sellers. 2014. *The Climate Modelling Primer.* . 4. ed ed., Chicester:Wiley Blackwell. 5, 13, 14

Mogensen, Patrick Kofod, and Asbjørn Nilsen Riseth. 2018. "Optim: A Mathematical Optimization Package for Julia." *Journal of Open Source Software*, 3(24): 615. 47

Murdock, James. 2003. *Normal Forms and Unfoldings for Local Dynamical Systems. Springer Monographs in Mathematics*, New York, NY:Springer New York. 8

Nævdal, Eric, and Michael Oppenheimer. 2007. "The Economics of the Thermohaline Circulation—A Problem with Multiple Thresholds of Unknown Locations." *Resource and Energy Economics*, 29(4): 262–283. 4

Nordhaus, William. 2019. "Economics of the Disintegration of the Greenland Ice Sheet." *Proceedings of the National Academy of Sciences*, 116(25): 12261–12269. 5

Nordhaus, William D. 1992. "An Optimal Transition Path for Controlling Greenhouse Gases." *Science*, 258(5086): 1315–1319. 21, 22

Nordhaus, William D. 2014. "Estimates of the Social Cost of Carbon: Concepts and Results from the DICE-2013R Model and Alternative Approaches." *Journal of the Association of Environmental and Resource Economists*, 1(1): 273–312. 48

Nordhaus, William D. 2017. "Revisiting the Social Cost of Carbon." *Proceedings of the National Academy of Sciences of the United States of America*, 114(7): 1518–1523. 22

Pindyck, Robert S, and Neng Wang. 2013. "The Economic and Policy Consequences of Catastrophes." *American Economic Journal: Economic Policy*, 5(4): 306–339. [4], [19], [20], [24]

Rackauckas, Christopher, and Qing Nie. 2017. "Adaptive Methods for Stochastic Differential Equations via Natural Embeddings and Rejection Sampling with Memory." *Discrete and continuous dynamical systems. Series B*, 22(7): 2731. [47]

Riihelä, Aku, Ryan M. Bright, and Kati Anttila. 2021. "Recent Strengthening of Snow and Ice Albedo Feedback Driven by Antarctic Sea-Ice Loss." *Nature Geoscience*, 14(11): 832–836. [7]

Seaver Wang, A. Foster, E. A. Lenz, J. Kessler, J. Stroeve, L. Anderson, M. Turetsky, R. Betts, Sijia Zou, W. Liu, W. Boos, and Z. Hausfather. 2023. "Mechanisms and Impacts of Earth System Tipping Elements." *Reviews of Geophysics*. [2], [5], [7], [14]

Shi, Hao, Hanqin Tian, Naiqing Pan, Christopher P. O. Reyer, Philippe Ciais, Jinfeng Chang, Matthew Forrest, Katja Frieler, Bojie Fu, Anne Gädeke, Thomas Hickler, Akihiko Ito, Sebastian Ostberg, Shufen Pan, Miodrag Stevanović, and Jia Yang. 2021. "Saturation of Global Terrestrial Carbon Sink Under a High Warming Scenario." *Global Biogeochemical Cycles*, 35(10): e2020GB006800. [11]

Skiba, A. K. 1978. "Optimal Growth with a Convex-Concave Production Function." *Econometrica*, 46(3): 527. [5]

Smith, Christopher J., Piers M. Forster, Myles Allen, Nicholas Leach, Richard J. Millar, Giovanni A. Passerello, and Leighton A. Regayre. 2017. "FAIR v1.1: A Simple Emissions-Based Impulse Response and Carbon Cycle Model." [5]

Tsur, Yacov, and Amos Zemel. 1996. "Accounting for Global Warming Risks: Resource Management under Event Uncertainty." *Journal of Economic Dynamics and Control*, 20(6-7): 1289–1305. 4

Turetsky, Merritt R., Benjamin W. Abbott, Miriam C. Jones, Katey Walter Anthony, David Olefeldt, Edward A. G. Schuur, Charles Koven, A. David McGuire, Guido Grosse, Peter Kuhry, Gustaf Hugelius, David M. Lawrence, Carolyn Gibson, and A. Britta K. Sannel. 2019. "Permafrost Collapse Is Accelerating Carbon Release." *Nature*, 569(7754): 32–34. 7

Van den Bremer, Ton S., and Frederick Van der Ploeg. 2021. "The Risk-Adjusted Carbon Price." *American Economic Review*, 111(9): 2782–2810. 4

Van Der Ploeg, Frederick, and Aart De Zeeuw. 2018. "Climate Tipping and Economic Growth: Precautionary Capital and the Price of Carbon." *Journal of the European Economic Association*, 16(5): 1577–1617. 4, 19, 34

Van Westen, René M., Michael Kliphuis, and Henk A. Dijkstra. 2024. "Physics-Based Early Warning Signal Shows That AMOC Is on Tipping Course." *Science Advances*, 10(6): eadk1189. 14

Wagener, F. 2013. "Regime Shifts: Early Warnings." In *Encyclopedia of Energy, Natural Resource, and Environmental Economics*. 349–359. Elsevier. 5, 14

Wagener, Florian. 2015. "Economics of Environmental Regime Shifts." In *The Oxford Handbook of the Macroeconomics of Global Warming*. , ed. Lucas Bernard and Willi Semmler, 0. Oxford University Press. 5

Weitzman, Martin L. 2012. "GHG Targets as Insurance against Catastrophic Climate Damages." *Journal of Public Economic Theory*, 14(2): 221–244. 21

Weitzman, Martin L. 2014. "Fat Tails and the Social Cost of Carbon." *American Economic Review*, 104(5): 544–546. 19

A Solution to Maximisation

This appendix deals with the solution of the maximisation problem (30).

A.1 Simplifying Assumptions on the Decay Rate of Carbon

To reduce the state space, following Hambel, Kraft and Schwartz (2021), I make an assumption on the decay rate of carbon. The calibrated carbon decay δ_m, as a function of the carbon stored in sinks N_t, is illustrated in Figure 18. The calibration assumes a functional form

$$\delta_m(N_t) = a_\delta e^{-\left(\frac{N_t - c_\delta}{b_\delta}\right)^2}, \tag{35}$$

for parameters $a_\delta, b_\delta, c_\delta$.
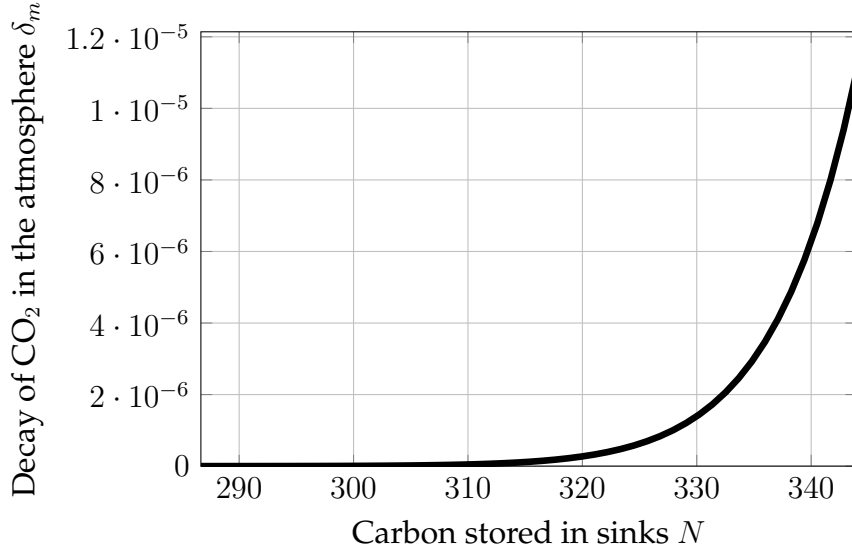
Figure 18: Estimated decay of carbon δ_m as a function of the carbon stored in sinks N_t.

I assume that the amount of carbon sinks present in the atmosphere is a constant fraction of the concentration in the atmosphere, $N_t = \frac{N_0}{M_0} M_t$. Abusing notation, I henceforth write $\delta_m(M_t)$ for the decay rate. Using this setup, under a business-as-usual emission scenario, the decay of carbon follows the path in Figure 19.
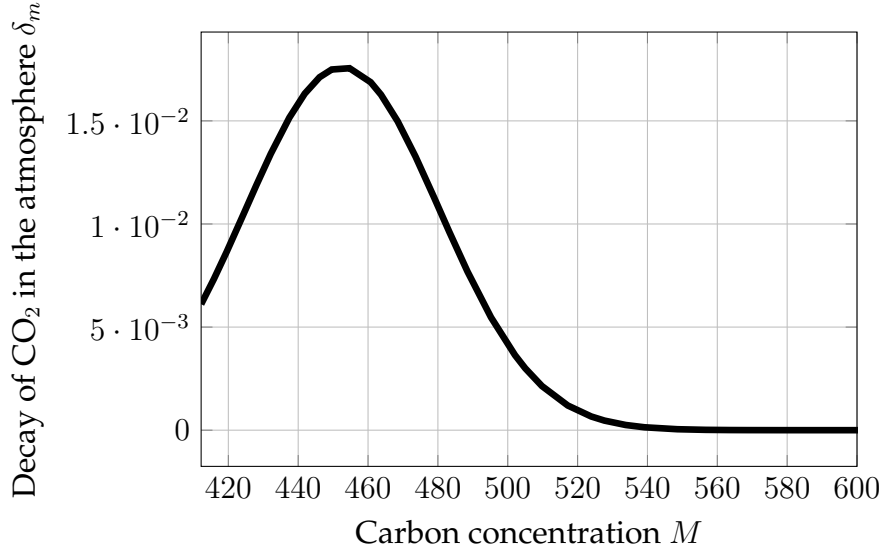
Figure 19: Estimated decay of carbon δ_m under the business as usual emission scenario M^b. Each marker is the decay after every decade.

A.2 Hamilton-Jacobi-Bellman equation

Using the assumption from Appendix A.1, the value function V at time t depends only on temperature T_t, log-carbon concentration m_t and output Y_t. This satisfies the Hamilton-Jacobi-Bellman equation

$$
\begin{aligned}
-\partial_t V = \sup_{\chi,\alpha} \; & f(\chi Y, V) + \partial_m V \,(\gamma_t^b - \alpha) + \partial_m^2 V \,\frac{\sigma_m^2}{2} \\
& + \partial_Y V (\varrho + \phi(\chi) - d(T) - \beta_t(\varepsilon(\alpha))) + \partial_k^2 V \,\frac{\sigma_Y^2}{2} \\
& + \partial_T V \,\frac{r(T) + g(m)}{\epsilon} + \partial_T^2 V \,\frac{(\sigma_T/\epsilon)^2}{2}.
\end{aligned}
\tag{36}
$$

It is easy to check that the ansatz

$$
V_t(T, m, Y) = \frac{Y^{1-\theta}}{1-\theta} F_t(T, m)
\tag{37}
$$

satisfies (36).

A.3 Approximating Markov Chain

The Hamilton-Jacobi-Bellman equation (36) is solved for F by adapting the method proposed in Kushner and Dupuis (2001). The idea is to discretise the state space of T and m and compute time dependent intervals $\Delta t(T, m)$. Then, constructing a Markov chain $\mathcal{M}$ over the discretised space, parametrised by some small step size h. Then we compute a discretised value function F^h with the property that $F^h \to F$ as $h \to 0$.

Given an h, construct a grid

$$\Omega_h = \{0, h, 2h, \ldots, 1-h, 1\}^2, \tag{38}$$

over the unit cube. This grid covers a suitable subset of the state space

$$\mathcal{X} := [T^p, T^p + \Delta T] \times [m^p, m^p + \Delta m] \tag{39}$$

where Δm is chosen such that $T^p + \Delta T$ is stable at $m^p + \Delta m$.

Using the ansatz (37) we can define a discrete value function F_t^h over the grid such that $F_t^h \to F_t$ as $h \to 0$ over χ, that is

$$
\begin{aligned}
F_t^h(T_t, m_t) = \min_{\chi, \alpha} \Bigg(& \left(1 - e^{-\rho \Delta t}\right) \chi^{1 - \frac{1}{\psi}} + \\
& e^{-\rho \Delta t} \left(\delta_y(\chi)\, \mathbb{E}_{t, \mathcal{M}(\alpha)} F_{t+\Delta t}^h(T_{t+\Delta t}, m_{t+\Delta t})\right)^{\frac{1 - \frac{1}{\psi}}{1 - \theta}} \Bigg)^{\frac{1 - \theta}{1 - \frac{1}{\psi}}}
\end{aligned}
\tag{40}
$$

where

$$
\begin{aligned}
\delta_y(\chi) &:= \mathbb{E}_t \left[\left(\frac{Y_{t+\Delta t}}{Y_t}\right)^{1 - \theta} \right] \\
&= 1 + \Delta t (1 - \theta) \left(\varrho + \phi(\chi) - d(T_t) - \frac{\theta}{2} \sigma_k^2\right) + \mathbb{E}_t \left[o(\Delta t^{\frac{3}{2}})\right].
\end{aligned}
\tag{41}
$$

and $\mathbb{E}_{t, \mathcal{M}(\alpha)}$ is the expectation with respect to the Markov chain $\mathcal{M}(\alpha)$ over the grid. This can be constructed, given a step size h, as follows. Introduce the

normalising factor

$$Q_t(T, m, \alpha) := \left(\frac{\sigma_T}{\epsilon \Delta T}\right)^2 + \left(\frac{\sigma_m}{\Delta m}\right)^2 + h\left|\frac{r(T) + g(m)}{\epsilon \Delta T}\right| + h\left|\frac{\gamma_t^b - \alpha}{\Delta m}\right|. \qquad (42)$$

Then the probabilities of moving from a point (T, m) of the grid to an adjacent point are given by

$$p(T \pm h\Delta T, m \mid T, m) \propto \frac{1}{2}\left(\frac{\sigma_T}{\epsilon \Delta T}\right)^2 + h\left(\frac{r(T) + g(m)}{\epsilon \Delta T}\right)^{\pm} \quad \text{and} \qquad (43)$$

$$p(T, m \pm h\Delta m \mid T, m) \propto \frac{1}{2}\left(\frac{\sigma_m}{\Delta m}\right)^2 + h\left(\frac{\gamma_t^b - \alpha}{\Delta m}\right)^{\pm} \qquad (44)$$

where $(\cdot)^+ := \max\{\cdot, 0\}$ and $(\cdot)^- := -\min\{\cdot, 0\}$. One can readily check that this is a well defined probability measure. Finally, the time step is given by

$$\Delta t = h^2/Q_t(T, m, \alpha), \qquad (45)$$

which satisfies $\Delta t \to 0$ as $h \to 0$.

Then, as the aggregator used in (40) converges to f (31) (Epstein and Zin, 1989), the chain described here satisfies the convergence properties outlined in Kushner and Dupuis (2001), we have $F_t^h \to F_t$ as $h \to 0$.

The Markov chain defined above allows to derive $F_t^h(T_t, m_t)$ from the subsequent $F_{t+\Delta t}^h(T_{t+\Delta t}, m_{t+\Delta t})$. This requires a terminal condition $\bar{F}^h(T_\tau, m_\tau) := F_\tau^h(T_\tau, m_\tau)$. To derive this, assume that at some point in a far future $\tau \gg 0$, the abatement is free and all emissions are abated, $\gamma^b = \alpha$, such that $\mathrm{d}m = \sigma_m \, \mathrm{d}W_m$. Then we construct an equivalent, control independent, Markov chain $\bar{\mathcal{M}}$ as above for

$$\bar{F}^h(T_t, m_t) = \min_\chi \left(\left(1 - e^{-\rho\Delta t}\right) \chi^{1 - \frac{1}{\psi}} + \right.$$
$$\left. e^{-\rho\Delta t} \left(\delta_y(\chi) \, \mathbb{E}_{t, \bar{\mathcal{M}}} \bar{F}^h(T_{t+\Delta t}, m_{t+\Delta t})\right)^{\frac{1 - \frac{1}{\psi}}{1 - \theta}} \right)^{\frac{1 - \theta}{1 - \frac{1}{\psi}}}. \qquad (46)$$

This is now a fixed point equation for $\bar{F}$ which can be solved by value or policy

function iteration.

A.4 Parallelisation

When computing the backward recurrence (40), each grid point $X_i \in \mathcal{X}$ is assigned a different time step $\Delta t(X_i)$, which depends on the curvature of the drift at that state. To parallelise the computation, I leverage the ZigZag algorithm by Bierkens, Fearnhead and Roberts (2019). Given the value function F_t^h, for a step back $t - \min_i \Delta t(X_i)$, I construct a directed graph among grid points $\mathcal{X}$ where an edge $X_i \to X_j$ is drawn if there is a positive probability of transitioning from X_i to X_j under the Markov Chain $\mathcal{M}$. This allows to obtain, at each point in time t, sets of points $\mathcal{C}_t \subseteq \mathcal{X}$ which are independent and over which it is possible to parallelise. The parallelisation is then conducted on the Snellius, the national high performance computer of the Netherlands. The algorithm is written in the `Julia` programming language and relies on `Optim.jl` (Mogensen and Riseth, 2018) and `StochasticDifferentialEquations.jl` (Rackauckas and Nie, 2017).

B Certainty Equivalence

This appendix defines the certainty equivalence, which allows to translate net present values to monetary values in the context of our problem. Let $X_t :=$ (T_t, M_t, N_t, Y_t) be the state at time t and denote by $\overline{\mu}$ and $\underline{\mu}$ the drift functions of X_t under a remote and an imminent tipping point respectively. Such that, in case of remote tipping,

$$\mathrm{d}\overline{X}_t = \overline{\mu}_t(X_t)\,\mathrm{d}t + \Sigma\,\mathrm{d}W_t \text{ where} \tag{47}$$

$$\Sigma := \mathrm{diag}(\sigma_T/\epsilon, \sigma_m, 0, \sigma_k) \tag{48}$$

and $\mathrm{d}W_t$ is a standard Wiener process. Under these dynamics, one can obtain the net present value in utils of the consumption stream $\overline{V}_0$ and $\underline{V}_0$ satisfying

equation (30). In a similar way one can compute the net present value of the consumption stream in utils of the wishful thinker (w) and prudent (p) policies as

$$V_0^i = \mathbb{E}_t \int_0^\infty f(Y_t \chi_t^i, V_t^i) \, \mathrm{d}t \tag{49}$$

with $i \in \{w, p\}$. For each $V \in \{\overline{V}, \underline{V}, V^w, V^p\}$, the corresponding certainty equivalent CE solves

$$V_0^i = f(CE, V_0^i). \tag{50}$$

C   Calibration and Parameters

This section summarises the parameters for the preferences, economy, and climate model and discusses the calibration strategy.

The following Table 3 illustrates the preferences parameters used throughout the paper. There is no consensus in the literature on preference parameters. In line with previous literature focusing on recursive preferences, I set relative risk aversion $\theta = 10$ (Ackerman, Stanton and Bueno, 2013; Crost and Traeger, 2013; Lontzek et al., 2015) and the time preference parameter $\rho = 1.5\%$ (Nordhaus, 2014). Following Hambel, Kraft and Schwartz (2021) I choose $\psi = 0.75$.

Preferences		
ρ	1.5%	Time preference
θ	10	Relative risk aversion
ψ	0.75	Elasticity of intertemporal substitution

Table 3

Table 4 summarises the parameters of the economy model. The calibration of these parameters reproduces that of Hambel, Kraft and Schwartz (2021).

Economy		
ω_0	11%	GDP loss required to fully abate today
ω_r	2.7%	Rate of abatement cost reduction
ϱ	0.9%	Growth of TFP
κ	6.32%	Adjustment costs of abatement technology
δ_k	0.0116	Initial depreciation rate of capital
ξ	0.00026	Coefficient of damage function
ν	3.25	Exponent of damage function
A_0	0.113	Initial TFP
Y_0	75.8 [trUS$/y]	Initial GDP
σ_k	0.0162	Variance of GDP
τ	500 [y]	Steady state horizon

Table 4

Table 5 summarises the parameters of the climate model.

Climate		
T_0	15.14 [°C]	Initial temperature
T^{p}	14 [°C]	Pre-industrial temperature
M_0	410 [p.p.m.]	Initial carbon concentration
M^{p}	280 [p.p.m.]	Pre-industrial carbon concentration
N_0	286.65543 [p.p.m.]	Initial carbon in sinks
σ_T	1.5844	Volatility of temperature
S_0	342 [W m^{-2}]	Mean solar radiation
ϵ	15.844 [J m^{-2} K y]	Heat capacity of the ocean
η	$5.67e - 8$	Stefan-Boltzmann constant
G_1	20.5 [W m^{-2}]	Effect of CO_2 on radiation budget
G_0	150 [W m^{-2}]	Pre-industrial GHG radiation budget

Table 5

Table 6 summarises the parameter of the temperature feedback.

Imminent		
T^c	1.5 °	Critical Temperature
$1/L_1$	1.8 °	Inverse speed of feedback kick-in
λ_1	0.31	Initial radiation reflected
$\Delta\lambda$	0.0326	Magnitude of feedback
Remote		
T^c	2.5 °	Critical Temperature
$1/L_1$	1.8 °	Inverse speed of feedback kick-in
λ_1	0.31	Initial radiation reflected
$\Delta\lambda$	0.0332	Magnitude of feedback

Table 6

D   Stochastic Tipping Benchmark Model

This appendix introduces a benchmark model with stochastic tipping. The stochastic tipping model is a widely used in the economic literature to approximate tipping points in the climate dynamics (e.g. Hambel, Kraft and Schwartz 2021). Comparing the model developed in this paper with the stochastic tipping model allows us to determine if and how the optimal abatement differ and, as a consequence, what the approximation misses.

To establish a meaningful benchmark, I will assume that the contribution of temperature to forcing (15) is given by

$$r_T^l(T_t) := S_0(1 - \lambda_1) - \eta\sigma T_t^4. \tag{51}$$

This model has no tipping point as $\lambda(T_t) \equiv \lambda_1$. Stochastic tipping, as commonly modelled in the literature, is introduced as a jump process J_t with arrival rate $\pi(T_t)$ and intensity $\Theta(T_t)$, both increasing in temperature. Intuitively, as temperature rises, the risk of tipping $\pi(T_t)$ and the size of the temperature increase

$\Theta(T_t)$ grow. Then temperature dynamics in the Stochastic Tipping model follow

$$\epsilon \, \mathrm{d}T_t = r^l(T_t) \, \mathrm{d}t + g(m) \, \mathrm{d}t + \sigma_T \, \mathrm{d}W_{s,t} + \Theta(T_t) \, \mathrm{d}J_t \tag{52}$$

where W_s is a Wiener process. Following Hambel, Kraft and Schwartz (2021), the calibrated arrival rate and temperature increase are calibrated as

$$\pi(T_t) = -\frac{1}{4} + \frac{0.95}{1 + 2.8e^{-0.3325(T_t - T_t^{\mathrm{P}})}} \text{ and} \tag{53}$$

$$\Theta(T_t) = -0.0577 + 0.0568(T_t - T_t^{\mathrm{P}}) - 0.0029(T_t - T_t^{\mathrm{P}})^2. \tag{54}$$